How paleosols influence groundwater flow and arsenic pollution: A model from the Bengal Basin and its worldwide implication

J. M. McArthur,[1] P. Ravenscroft,[2] D. M. Banerjee,[3] J. Milsom,[1] K. A. Hudson-Edwards,[4] S. Sengupta,[5] C. Bristow,[4] A. Sarkar,[5] S. Tonkin,[1] and R. Purohit[3]

Received 27 September 2007; revised 14 July 2008; accepted 28 July 2008; published 8 November 2008.

[1] In the Bengal Basin, the land surface exposed during the last lowstand of sea level around 20 ka, and now buried by Holocene sediment, is capped by an effectively impermeable clay paleosol that we term the Last Glacial Maximum paleosol (LGMP). The paleosol strongly affects groundwater flow and controls the location of arsenic pollution in the shallow aquifers of our study site in southern West Bengal and, by implication, in shallow aquifers across the Bengal Basin and As-polluted deltaic aquifers worldwide. The presence of the LGMP defines paleointerfluvial areas; it is absent from paleochannel areas. A paleosol model of pollution proposed here predicts that groundwater in paleochannels is polluted by arsenic, while that beneath paleointerfluvial areas is not: paleointerfluvial aquifers are unpolluted because they are protected by the LGMP from downward migration of arsenic and from downward migration of organic matter that drives As-pollution via reductive dissolution of As-bearing iron oxyhydroxides. Horizontal groundwater flow carries arsenic from paleochannels toward paleointerfluvial aquifers, in which sorption of arsenic minimizes the risk of pollution.

Citation: McArthur, J. M., P. Ravenscroft, D. M. Banerjee, J. Milsom, K. A. Hudson-Edwards, S. Sengupta, C. Bristow, A. Sarkar, S. Tonkin, and R. Purohit (2008), How paleosols influence groundwater flow and arsenic pollution: A model from the Bengal Basin and its worldwide implication, *Water Resour. Res.*, *44*, W11411, doi:10.1029/2007WR006552.

1. Introduction

[2] In the Bengal Basin, the health of domestic consumers of groundwater has been adversely affected by arsenic pollution [*Dhar et al.*, 1997; *Smith et al.*, 2000; *Saha and Chakraborti*, 2001; *Chakraborti et al.*, 2003; *Ravenscroft et al.*, 2009]. Although the distribution of arsenic pollution in wells is known spatially, from studies in both West Bengal [*Public Health Engineering Department*, 1991; *Das et al.*, 1996] and Bangladesh [*Department of Public Health Engineering* (*DPHE*), 1999, 2001; *van Geen et al.*, 2003], the role played by sedimentology and groundwater flow in affecting that distribution is not known well.

[3] The first large-scale survey of arsenic pollution in groundwater of Bangladesh [*DPHE*, 1999] showed that it was apparently confined to aquifers of gray sand formed after the lowstand of sea level at the Last Glacial Maximum (LGM) around 20 ka. Arsenic pollution was also noted by *DPHE* [1999] to be essentially absent from the underlying, yellow/brown, Pleistocene aquifers that were typically found at depths >100 meters below ground level (mbgl). Further surveying confirmed those finding and repeated those conclusions [*DPHE*, 2001]. Mapping As pollution at a much finer spatial scale lead *McArthur et al.* [2004] to suggested that the distribution of permeability and organic matter, in the aquitard capping the shallow aquifer of southern West Bengal, might control arsenic distributions in groundwater. That view was prompted by their finding of an impermeable "brown clay" at around 21–24 mbgl in southern West Bengal that appeared a possible control on groundwater flow, and so on the distribution of arsenic.

[4] Here, we develop that idea and show that the "brown clay" noted by *McArthur et al.* [2004] is but a local representation of a basin-wide (indeed, a global) event. The "brown clay" is identified as a paleosol horizon and is shown here to be present widely in the study region and, by implication, elsewhere. It formed by weathering of the exposed land surface as sea level fell during the Pleistocene, albeit with reversals, from a high at 125 ka to a low of around 120 mbsl at 20 ka [*Umitsu*, 1993; *Lambeck et al.*, 2002]. The fall was glacioeustatic; that is, it was a global fall in sea level. The glacial culmination, and so the lowest stand of sea level, occurred at around 20 ka and is commonly termed the Last Glacial Maximum. We therefore term the paleosol the Last Glacial Maximum paleosol (LGMP) while acknowledging this to be shorthand for its extended development. The presence of this paleosol, or its absence through nondeposition or erosion, has a strong control on groundwater flow and so on the distribution of

[1]Department of Earth Sciences, University College London, London, UK.
[2]Department of Geography, University of Cambridge, Cambridge, UK.
[3]Department of Geology, University of Delhi, Delhi, India.
[4]School of Earth Science, Birkbeck University of London, London, UK.
[5]Department of Geology and Geophysics, Indian Institute of Technology, Kharagpur, India.

0043-1397/08/2007WR006552

arsenic pollution in our field area in West Bengal. We explore this control by relating aquifer sedimentology to the distribution of arsenic in groundwater, and by exploratory modeling of groundwater flow using MODFLOW. We show, by reference to published works, that the LGMP is present widely across the Bengal Basin. The paleosol caps the underlying aquifer, which contains low-As groundwater, and so protects it from vertical migration of arsenic and organic matter. The paleosol does not protect the unpolluted aquifer from lateral invasion at depth by As pollution and organic matter: we attempt to estimate the risk posed by this lateral invasion to the reserves of low-As water.

[5] Finally, we explore a corollary of the oft-quoted statistic that some 25% of wells in the Bengal Basin are polluted with more than 50 μg/L of arsenic [*DPHE*, 1999, 2001]. The corollary is that 75% of wells are not polluted by arsenic, if that benchmark is used. Application across the Bengal Basin of our paleosol model for arsenic distribution may provide an explanation of why many aquifers are not polluted; the protection afforded by the LGMP to underlying aquifers that keeps such brown sands brown and unpolluted. The identification of the LGMP by drilling and geophysical exploration offers a practical prospect of locating long-term supplies of low-As water at shallow depth across the entire Bengal Basin.

[6] The LGMP may be a strong control of flow within deltaic aquifers worldwide, because the sea level low at the Last Glacial Maximum occurred worldwide. Paleosol formation at that time must also have been worldwide. Our findings therefore have important implications for water supply in deltaic aquifers everywhere, because shallow, As-free tube wells provide a cheap and safe source of drinking water across the Bengal Basin, in partly polluted aquifers elsewhere in India, and in Pakistan, Vietnam, Cambodia, Myanmar, China, Taiwan, and Japan.

2. Study Area

[7] The study area is that described by *McArthur et al.* [2004], plus a substantial extension northward (Figure 1). It comprises the villages of Joypur, Ardevok, and Moyna and the area to the north, which we together term JAM. The site is in southern West Bengal at 22° 44.43 N, 88° 29.45′ E (Indian/Bangladesh datum) in 24-Parganas (North) district. The area includes agricultural land in the north and village habitation in the south. The agricultural land grows rice, vegetables, and pulses with and without irrigation. The climate is tropical monsoonal, with a dry season between November and May. Rainfall is typically 1300 mm/a. Most rain falls in the monsoon between June and October [*Sengupta and Sarkar*, 2006]. Survey of India topographic maps show the study area to be around 7–8 m above mean sea level.

[8] The alluvial aquifer is recharged only from rainfall. In the village area and to its south there are numerous artificial ponds (Figure 1) but they contribute little to recharge [*Sengupta et al.*, 2008]. Ponds are never overtopped during rain. The Hoogli River flows from north to south some 13 km to the west of the area, but is too far away to contribute to recharge, given that the region has a relief of less than a few meters, and the seasonal change in the level of groundwater is <5 m. The Sunti River (now ponded and not flowing) runs from south to north along the eastern margin of JAM (Figure 1), joining the east-west trending Sunti Channel (also ponded and nonflowing) about 0.5 km to the north of our area.

[9] The area is underlain by a shallow aquifer, around 30–40 m thick, in which groundwater contains <10–1410 μg/L of arsenic. The shallow aquifer is overlain by organic-rich silts and clays that vary in thickness (6–21 m) across the study area. The shallow aquifer is underlain by an impermeable clay some 20 m thick that separates it from a deep aquifer, at >70 mbgl, that is not polluted by arsenic. Water for irrigation comes from ponds, private wells that tap the shallow aquifer, and two high-capacity public tube wells that have tapped the deep aquifer at a depth of 175 mbgl since 1970 (Figure 1). Water for domestic use is drawn from hand-pumped tube wells, some 95% of which tap the shallow aquifer (see *McArthur et al.* [2004], for details).

3. Methods

[10] We defined the stratigraphy of the region through a combination of shallow-resistivity survey, drilling, and coring, and we defined directions of groundwater flow through piezometric monitoring. We sampled groundwater from irrigation wells and new observation wells drilled for this study in order to define the areal distribution of arsenic pollution and the variability of sediment character. We dated sediments with ^{14}C and by the optically stimulated luminescence (OSL) method.

[11] To investigate the stratigraphy and to obtain sediment for investigation, we drilled eight boreholes in 2004 to around 50 mbgl (SW1–SW8 on Figure 1). The logs from these drillings supplemented cores and logs from 24 boreholes drilled in 2003 to make three multilevel piezometer nests (AP, DP and FP in Figure 1; for details, see *McArthur et al.* [2004]). Most sediment samples were obtained using the manually operated, reverse circulation, percussion method [*Ali*, 2003]; cohesive sediment returns as slightly disturbed cores, noncohesive (sandy) sediment returns as slurry. Samples were collected after decanting supernatant following a brief period of settling; samples were not washed further. Piezometers were 38 mm diameter PVC casing; the bottom 1.5 m was machine slotted to act as a well screen. The annular space around the well screen was filled with clean, coarse, sand and sealed above with bentonite. At piezometer site AP we obtained cores for dating by OSL. Coring was by the percussion method using a solid-wall core barrel enclosing a PVC liner. Core barrels were opened in complete darkness, core tubes capped, and cores wrapped in multiple layers of aluminum foil and black plastic for transport to the OSL laboratory.

[12] To extend the findings from drilling, apparent resistivity was measured in February 2004 along N–S and E–W lines of traverse across the field area. We used a Geopulse DC meter and a Wenner electrode array with separations of 8, 16, and 32 m. In addition, to obtain more detailed resistivity-depth functions, we ran two expanding arrays using separations of 1, 2, 3, 5, 7, 10, 15, 20, 30 and 48 m.

[13] To assist in sediment characterization and lithostratigraphic correlation, we determined the chemical compositions of sediments using by ICP-AES after total dissolution of sediment in $HClO_4$/HF and take-up of residues in 2% HNO_3. Concentrations of SiO_2 were determined by ICP-AES on samples fused with lithium metaborate and taken

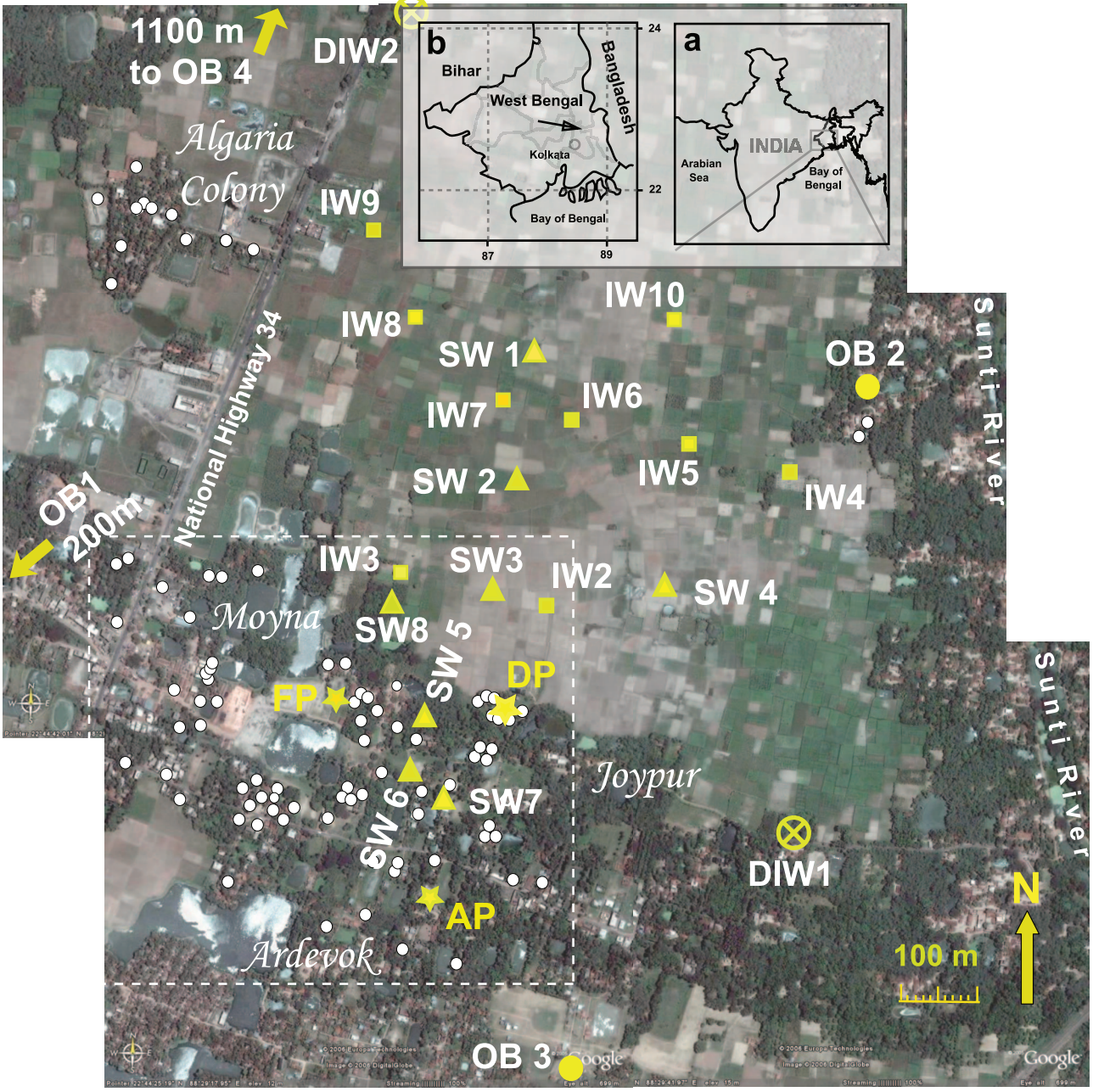

Figure 1. The study area. Comparison with spot heights on Survey of India topographic sheets suggests a ground elevation of 7–8 m above mean sea level (amsl). The white dashed box outlines the study area of *McArthur et al.* [2004]. Small white circles show locations of wells for which chemical composition is reported by *McArthur et al.* [2004]. Wells SW1–4 and SW8 (yellow triangles) were installed in the near field to reveal sedimentology and to provide observation wells. Boreholes SW5, 6, and 7 are holes drilled to reveal sedimentology. OB1–4 (large yellow circles) are observation wells in the far field used to monitor water level. Yellow stars are piezometer nests installed to monitor water level and composition in the inner field (see Table S2 for data). Squares are private irrigation wells in the shallow aquifer (for depths, see Table 3). DIW1 and DIW2 are deep wells of large capacity used for irrigation in the area via a buried pipe system. Base map from Google Earth, copyright 2006 Europa Technologies, 2006 DigitalGlobe, used with permission.

up in 2% HNO_3. To quantify the amount of organic matter in sediments that might drive subsurface redox reactions, we also measured total carbon (TC) and total sulfur (TS), and total organic carbon (TOC; after decarbonating samples with 10% HCl) using a ®LECO C/S analyzer. Concentrations of calcite were determined by difference between TC and TOC.

[14] Using the radiocarbon method (Beta Analytical, Miami, Florida) we dated 12 samples of peat, wood and organic-rich sediment from AP, FP and DP (Figure 1). Calendar years before present (BP, i.e., before 1950) were derived from the calibrations of *Talma and Vogel* [1993], *Stuiver and van der Plicht* [1998], and *Stuiver et al.* [1998]. Optically stimulated luminescence (OSL) dates were obtained on 6 samples of quartz, using the methods of *Murray and Wintle* [2000], *Bray et al.* [2002], *Bray and Stokes* [2003, 2004], and *Bailey et al.* [2003]. The intensity of OSL emission was measured after excitation with light of wavelength 470 nm ($P_{max} \sim 18$ mW cm^{-2}). To correct for sensitivity changes during cycles of dose-preheat-optical stimulation, a 1 Gray test dose was given. To determine the effectiveness of the sensitivity correction (recycling ratio), the initial regeneration point was repeated [*Murray and Wintle*, 2000]. Dose rates were calculated using K, U and Th concentrations determined by the method of *Bailey et al.* [2003]. A cosmic dose of 0.19 Gray/ka and a moisture value of 0.3 were used to construct age models for the samples.

[15] Groundwaters were collected from irrigation wells IW2–11 and observations wells SW1–4 and SW6–8 (Figure 1) in polyethylene sample tubes after purging the boreholes. Samples without turbidity (almost all) were not filtered; samples with turbidity were filtered on site through 0.45 μm acetate membrane filters. Samples for cation analysis were acidified in the field with Analar® nitric acid to make them 1.5% acid; samples for anion analysis were not acidified. Analysis for cations was done using a Perkin-Elmer ICP-AES. Analysis for anions was done using a Dionex ion chromatograph. Precision was better than 5% in both cases as judged by replicate analysis.

[16] Piezometers and observation wells (drilled 2003 and 2004; Figure 1) were surveyed to a local site datum using either optical or laser theodolite. Repeat surveys showed that levels are reproducible to better than 1 cm. The water levels in these near-field wells were measured with an electrical dipper at intervals of two to three month intervals for 2 years. All measurements were completed within a few hours on the same day in order to minimize inaccuracy caused by local daily drawdowns of several centimeters noted elsewhere by *Harvey et al.* [2006] as resulting from large-scale irrigation pumping. Such variation was seen in our area when repeat measurement was made over periods of days (see auxiliary material, Table S2).[1] To measure water levels in the far field, four additional observation boreholes (OB1–4; Figure 1) were surveyed in to the local site datum in 2005 and water levels were measured in 2005 and 2006. Water level measurements for these far-field wells were completed in less than 1 day with a minimum of delay, but may be marginally affected by daily drawdown artifacts.

[17] In February 2004, rising- or falling-head measurements of hydraulic conductivity were made at each piezometer using a solid, 30-cm-long slug. During the tests, water levels were measured at intervals from 0.5 to 10 s with a Van Essen pressure transducer. Tests on low-permeability units showing underdamped responses were interpreted using the *Bouwer and Rice* [1976] method as implemented in the AQTSOLV® program [*HydroSOLVE*, 1999]. Tests on high-permeability units showing overdamped responses were interpreted using the *van der Kamp* [1976] method as implemented in the spreadsheet of *Halford and Kuniansky* [2002]. Pumping tests, discharging up to 0.36 l/s, were conducted on one piezometer at each piezometer nest to assess the vertical continuity of the aquifer-aquitard sequence. Water levels were recorded at 1s intervals with pressure transducers, supplemented by manual measurements. Pumping times were 60–90 min. Water was discharged to ground 5–10 m away from the well. Time-drawdown and distance-drawdown data were interpreted using the Cooper-Jacob and Theis recovery methods [*Kruseman and de Ridder*, 1992].

4. Results and Outline Interpretation

4.1. Lithology and Hydrostratigraphy

[18] Drilling revealed seven stratigraphic units, which are given informal stratigraphic names based on local place names. One unit, the deep aquifer at depths >70 mbgl, is not the subject of this study. The main features of, and spatial relation between, the other six units are shown in Figures 2 and 3. The units are arranged into two distinct sequences. One sequence, found at DP, SW2, SW3, SW4, SW6, and SW8 (Figure 1) comprises around 20 m of organic-rich, peaty silts and muds floored by a stiff blue-gray clay: beneath the blue-gray clay lies an orange/brown, sometimes mottled, stiff clay, which grades downward into brown sands >30 m thick. The other sequence, found at AP, FP, SW1, SW5, and SW7 (Figure 1), is less rich in organic matter and comprises around 10 m of silty muds over two units of gray sand: the sand units differ in age, composition, and provenance and are separated by an unconformity. Both sequences are floored by a stiff gray clay some 20 m thick. From base to top, the units and the names we assign are as follows.

[19] The Sunti Formation comprises the deep aquifer, of thickness >100 m, and the overlying Sunti Clay Member that is 20 m thick. The uppermost few decimeters of the Sunti Clay Member is light brown in color and oxidized. The unit is overlain by the Moyna Member and the laterally adjacent Ardevok Member of the Barasat Formation. The Moyna Member comprises brown sands capped by a stiff, orange/brown clay (the "brown clay" of *McArthur et al.* [2004]) that is typically 2–3 m thick; this clay contains carbonized rootlets (Figure 4) that show it to be a paleosol; it is termed here the Last Glacial Maximum paleosol (LGMP). The Ardevok Member is mostly gray sand but, locally (e.g., at AP and SW7), may have 1–2 m of brown sand at the base.

[20] The Barasat Formation is overlain by sands, muds and silts of the Joypur Alluvium. The uppermost unit, the Hoogli Member, consists of organic-rich peaty silt. Where the LGMP is present, it is directly overlain by the Hoogli Member, and that member is floored by a pale blue-gray clay around 1 m in thickness (Figures 2 and 4). This clay passes upward into a few meters of silt, before peat appears in some bores around 15 mbgl. The blue-gray clay may have been deposited as sea level rise, post-LGM, overtopped the interfluves, or it may represent an upper part of

[1] Auxiliary material data sets are available at ftp://ftp.agu.org/apend/wr/2007wr006552. Other auxiliary material files are in the HTML.

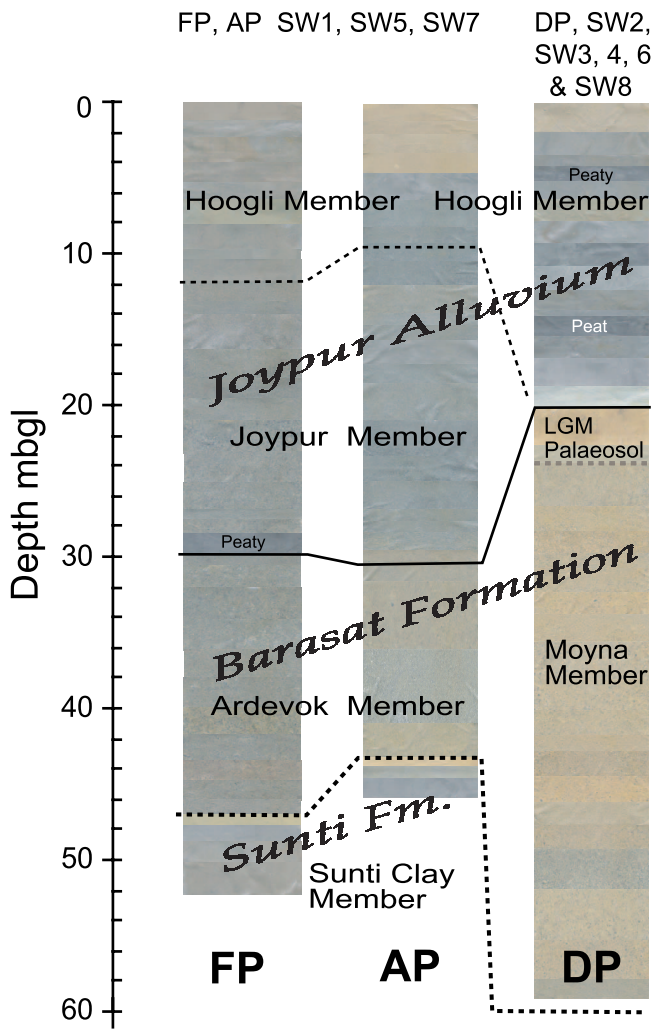

Figure 2. Color logs of the two contrasting sedimentary sequences seen in the study area (JAM), showing major lithological units, the stratigraphic names assigned here, and the color variation down core patched from electronic scans of wet samples. Cores taken at AP and FP are representative of cores from SW1, SW5, and SW7. The core from DP is representative of cores taken at SW2, SW3, SW4, SW6, and SW8. The uppermost few decimeters of the Sunti Clay Member are oxidized and are light brown in color.

the LGMP that has suffered reduction since burial by organic-rich fluids derived from overlying peat. Where the LGMP is absent, the Hoogli Member is underlain by the Joypur Member of dark, micaceous, gray sand, which sits directly on top of the dominantly gray sand of the Ardevok Member of the underlying Barasat Formation. Locally (e.g., at FP, and in two boreholes within 15 m), an organic-rich unit 50 cm thick (7% TOC [*McArthur et al.*, 2004]) separates the Barasat Formation and the Joypur Alluvium.

[21] While the lithological units described above are consistently recognizable in cores, a different classification of the subsurface is more suited at times to discussion of groundwater flow. This hydrostratigraphic nomenclature renames the Sunti Clay Member as the lower aquiclude, because it forms an impermeable base to the shallow aquifer. Sands of the Moyna, Ardevok, and Joypur members are renamed the shallow aquifer, and the silts of the Hoogli Member are termed the upper aquitard, because they cap the entire study area.

4.2. Geophysics

[22] The results of the multiseparation resistivity profiling are presented as pseudosections of apparent resistivity in Figure 5 and relate to the lines of survey shown in Figure 6. Measured apparent resistivity values are between 8 and 25 Ω m. The values are low, but the ratio between the highest and lowest was above the noise level of the measurements. A low-resistivity layer characterizes the middle part of the longest traverses (E–W line 00, and N–S line 288E), much of line 350N, the eastern end of line 100N, the southern end of line 350E, and the northern end of 250E. An expanding array run in the center of JAM (*E2* in Figures 5 and 6) shows an abrupt decline in apparent resistivity at separations of between 5 and 15 m, and low between 15 and 30 m separation, and an increase at the greatest separation of 48 m, revealing that a layer of low apparent resistivity occurs between two layers of higher resistivity. These results delineate a region centrally located within the study area where resistivity is low; we term this region the low-resistivity zone or LRZ. It occurs at shallow depth (Figure 5) but has no visible surface expression. To the west, north, and southwest, the LRZ pinches out and apparent resistivity is high at all depths. No data were collected to the east and southeast owing to constraints of time. An expander array in the northeast of JAM (*E1* on Figures 5 and 6) showed low resistivity (<12 Ω m) at all separations up to and including 20 m, after which there is a small increase to 16 Ω m at 48 m separation.

[23] Drilling showed that the prominent paleosol horizon (LGMP in Figures 2–4) and its overlying pale blue-gray clay, were found only beneath the low-resistivity zone, so we ascribe the low resistivity to the occurrence of these units. Typically, the depth of penetration of a Wenner array is half the electrode spacing, unless an especially conductive zone is present at greater depth to capture the current. Our maximum spacing was 32 m for the Wenner array, and 48 m for the expanding arrays. As clays conduct electricity well, we postulate that the clay of the LGMP, and the overlying meter of pale blue-gray clay, captured the majority of input current during the resistivity surveys. We therefore infer that the area of the LRZ coincides with the areal extent in the subsurface of the LGMP, which drilling found at a depth of 21–24 m.

4.3. Sediment Dating

[24] The ^{14}C dates and OSL dates obtained on sediment from AP, FP and DP (Figure 1) are given in Table 1. Where the same level yielded dates on both bulk organic matter dispersed in sediment, and discrete in situ fragments of wood or peat, the former are up to 300 years older, probably because of a reservoir effect that retains and recycles carbon during and after burial. For the OSL dates on quartz, many of the grains had been partially bleached during reworking; this has increased the uncertainties on the dates for some samples (Table 1). For APOSL 2, 3, 4, 5 uncertainties (95% confidence interval) are less than 10% of the minimum age. For APOSL 1 it is ±35%. Because of the partial bleaching, we use minimum estimates of age in our interpretation in

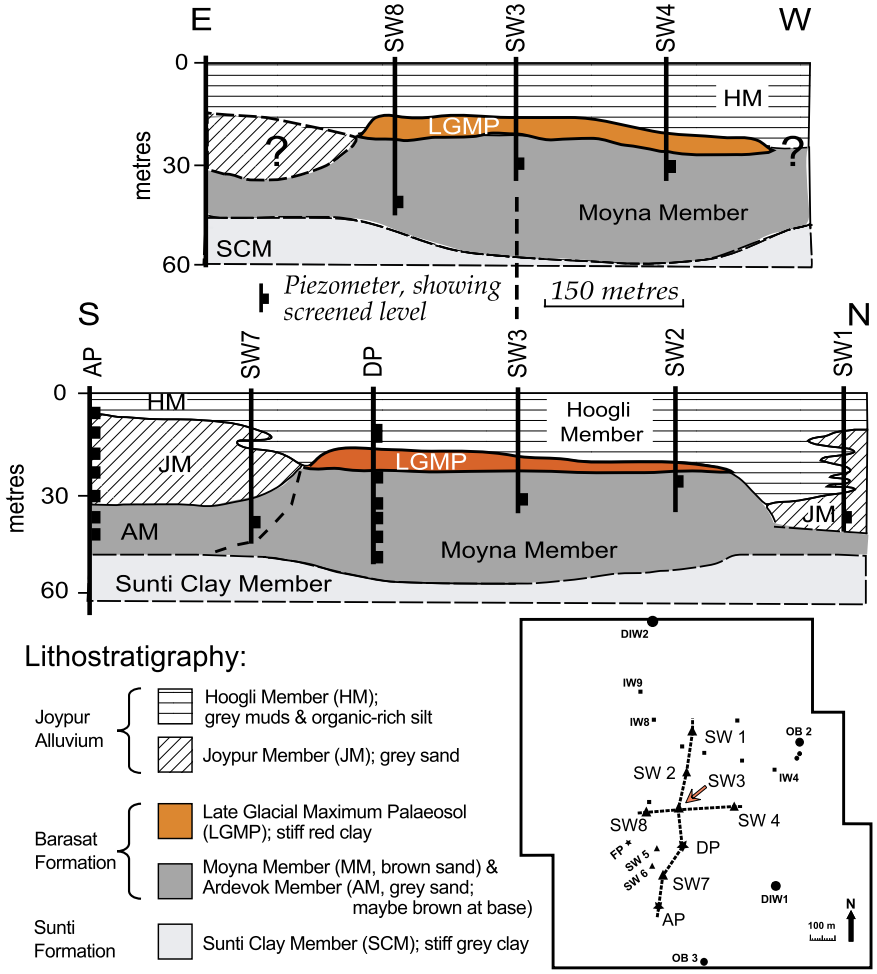

Figure 3. Geological cross section through the study area, based on apparent resistivity profiles and drilling. Drilling sites are shown with levels of screens. Inset shows lines of section.

preference to mean ages [cf. *Bray and Stokes*, 2004]. The OSL dates at AP are, despite these potential problems, in correct stratigraphic order and are consistent with the ^{14}C calendar ages.

[25] Organic matter from the unweathered part of the Sunti Clay Member, at 50 mbgl at FP, yielded a radiocarbon date of 27.2 ± 0.4 ka (the age is beyond the range of calendar year calibration) showing that this unit is latest Pleistocene in age, or older. This age is taken as the minimum age because the sample may have been contaminated with modern carbon by bacterial activity during sample storage.

[26] At AP, the boundary between the Joypur Member and the underlying Ardevok Member is marked by the increase in OSL dates from <8 ka above 32 mbgl to >17 ka below it, so we take the former to be Holocene and the latter to be Pleistocene. Such an interpretation is consistent with the occurrence in FP of an organic-rich unit at 29 mbgl, that separates the Joypur Member from the underlying Ardevok Member, and dates to 7.22 ± 0.04 ka with ^{14}C. The interpretation is also consistent with an increase in aquifer hardness around 32 mbgl in AP that was revealed by penetrometer testing during coring [*British Standards Institution*, 1975]. The three OSL dates between 31.5 and 19 mbgl at AP group tightly around 7.0 ka, a spread that suggest these Holocene sands of the Joypur Member form a homogeneous unit that was deposited in less than 1.0 ka at a time around 7 ka.

[27] The LGMP and Moyna Member were not dated directly. As the LGMP is the only paleosol within the sedimentary sequences we discuss, it must have formed during the long time interval between the sea level highstand at 125 ka and the time of its burial by younger Holocene sediments, possibly around 8 ka, as sea level rose after the LGM. Insofar as a paleosol may be said to have an "age," one of <20 ka for the LGMP is inconsistent with the age range of 17–23 ka for the Ardevok Member, which is derived from the Moyna Member on which the LGMP developed. It follows that the Moyna Member must be considerably older than 20 ka, and that the LGMP must have developed mostly in the interval between the sea level highstand around 125 ka and the LGM around 20 ka.

[28] For the Hoogli Member, sediment from 10 mbgl at AP, near its base (Figure 2), gave an OSL age of 3.8 ± 1.3 ka. At DP, where the unit is thicker, organic matter gave dates of 1.16 ka to 1.47 ka BP at 5.2 mbgl and 7.35 ka to 7.92 ka around 15 mbgl. Thus, the upper part of the unit formed in historical time, while the lower part may have been eroded (or was never deposited) in those regions now occupied by the sands of the Joypur Member. While most of the Hoogli Member is Holocene in age, we have little control on its age between 16.8 mbgl (^{14}C age of 7.9 ka;

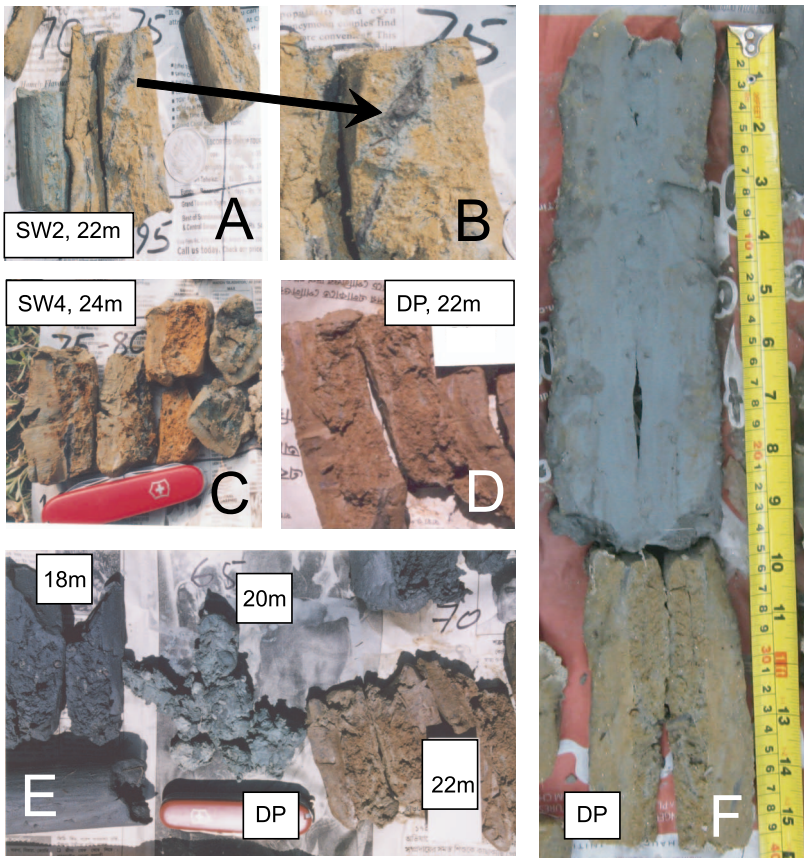

Figure 4. (a–e) The paleosol at around 24 mbgl is termed here the Last Glacial Maximum paleosol (LGMP in text). Scale is given by a coin in Figures 4a and 4b, a penknife in Figures 4c and 4e, and newsprint in Figure 4d. Note dark paleorootlets marked by the arrow in Figures 4a and 4b and the color variation of the LGMP between sites SW2, SW4, and DP. Lithologies overlying the LGMP are shown in Figure 4e: a peat horizon at 18 m, a pale blue-gray clay at 20 m, and the LGMP below. (f) Also shown is the contrast between the LGMP and the overlying pale blue-gray clay and the sharpness of the contact between them.

Table 1), and the base of the pale-blue clay around 21 mbgl. The few meters of silt and the pale-blue clay (if it is not a reduced upper portion of the LGMP) that overlie the LGMP were deposited after the LGM and before 7.9 ka, but when in that interval is neither certain, nor important to our study.

4.4. Sediment Composition

[29] The upper few decimeters of the Sunti Clay Member (the lower aquiclude) are oxidized, light brown in color, and contain little TOC and TS in comparison with underlying levels of gray clay (Figure 2 and Tables 2 and S1). The unoxidized, deeper, clay between 48.7 and 69.6 mbgl contains up to 1.3% TOC, and up to 1.6 % of pyritic sulfur (Figure 7 inset and TOC data for core FP in Data Set S1). The TOC and TS concentrations correlate and define a slope for C/S (wt % ratio) of around 1.1 (inset in Figure 7); values ≤ 2 indicate either a marine origin [*Berner and Raiswell*, 1984] or an origin as mangrove mud [*Woolfe et al.*, 1995]. The important conclusion to draw from these data is that the Sunti Clay Member was deposited at or below sea level.

[30] A notable feature of the chemical composition of the sands of the shallow aquifer (Moyna, Ardevok and Joypur members) is that the brown Pleistocene sands of the Moyna Member are chemically indistinguishable from the (mostly) gray Pleistocene sands of the Ardevok Member (Figure 7 and Table 2). The mean compositions of both Pleistocene units are, however, different from the mean composition of the gray Holocene sands of the Joypur Member (Figure 7), with the Pleistocene sands containing more SiO_2 but less of most other major and trace elements. The Holocene sands of the Joypur Member typically contain 5% calcite and 0.1–0.5% TOC, while Pleistocene sands of the Ardevok and Moyna members contain only trace amounts of calcite and around 0.1% TOC. The chemical similarity of the Moyna and Ardevok members of the Barasat Formation lead us to conclude that they are of related origin, as discussed below.

[31] Compared to the brown sand of the Moyna Member on which it sits, the red/orange clay of the LGMP is enriched in elements that are immobile during oxic weathering (e.g., Fe, Ni, Cr, V) and depleted in elements that are mobile during oxic weathering (Na, Li; see *Hill et al.* [2000] and *Kahmann et al.* [2008, and references therein] for a discussion of element mobility during weathering and paleosol formation). These enrichments and depletions accord with the conclusion, drawn from its oxidized coloration and its content of carbonized roots, that the LGMP is a weathered horizon i.e., a paleosol.

[32] The uppermost few meters of the Joypur Alluvium (Hoogli Member) are oxidized by modern weathering. The

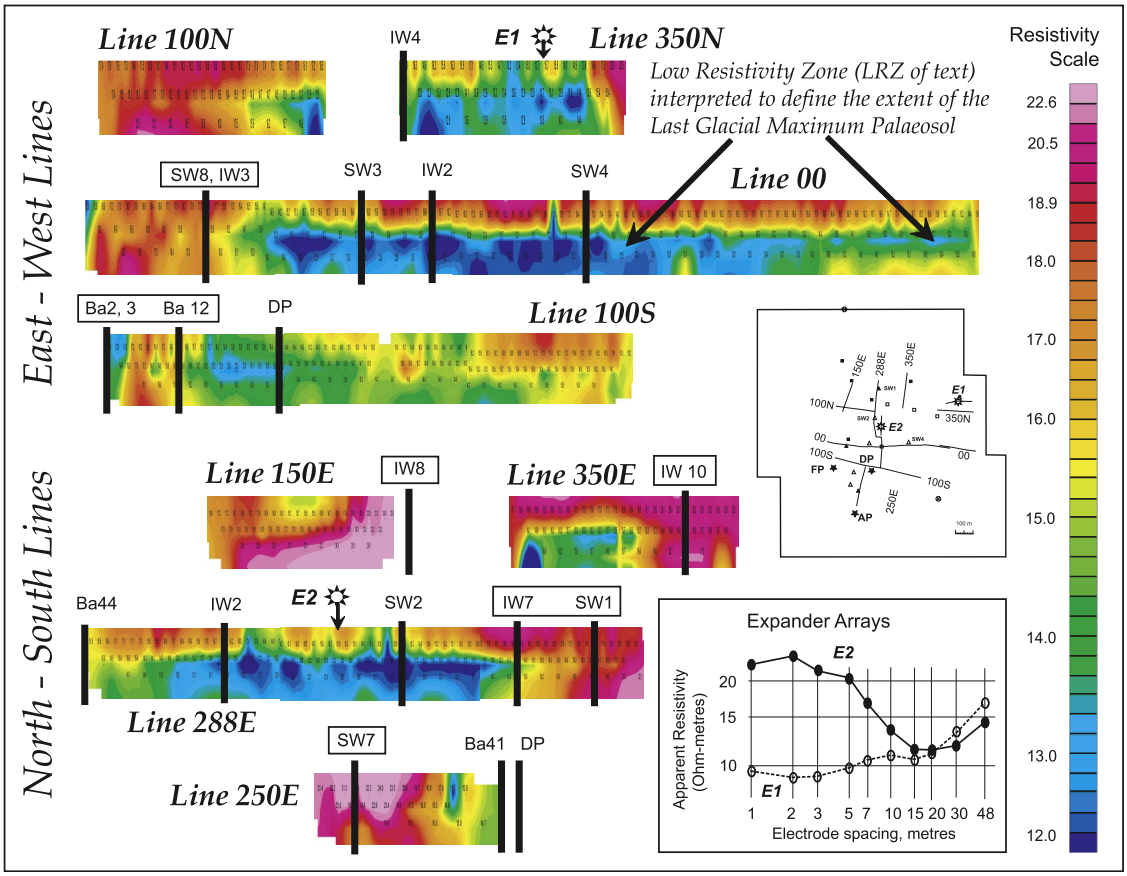

Figure 5. Distribution of apparent resistivity along the profile lines shown in Figure 6. The long lines (00 and 288E) show a low-resistivity zone (LRZ in text) at shallow depth. Lithologies revealed by drilling suggest that the LRZ comprises an impermeable clay paleosol horizon (LGMP in text) at around 24 mbgl and an overlying pale blue-gray clay (Figure 4), both of which capture current. Arsenic-polluted sites are denoted in the profiles by boxed numbers. Stars are sites of expander arrays for which resistivity data are shown in the bottom inset.

feature of most importance is the high TOC concentrations in the unweathered parts of this unit, in which organic matter (reported as TOC) ranges from 0.5% to 34% (Data Set S1) [see also *McArthur et al.*, 2004, Table 2]. The organic content of the Hoogli Member increases as its thickness increases; at DP, it contains at least three horizons of peat in the strict sense, with books of compressed decaying leaves found at various depths between 10 and 17 mbgl.

4.5. Hydrochemistry

[33] Although not discussed further, the deep aquifer yields water with $\leq$25 and mostly <10 μg/L As. All further discussion relates to groundwaters from the shallow aquifer. Compositional data of new wells drawing groundwater from the shallow aquifer and analyzed for this work are given in Table 3 and the geographical distribution of arsenic pollution of groundwater is shown in Figure 8. Chemical data for groundwaters from piezometers are reproduced from *McArthur et al.* [2004] in Table S1, and chemical compositions of other wells shown in Figure 1 as closed white symbols are given by *McArthur et al.* [2004]. All the groundwaters are anoxic; they contain either arsenic, together with iron in mg/L amounts but little manganese, or mg/L amounts of manganese but little arsenic or iron. A handful of wells yield groundwater that contains all three elements in substantial amounts. Such wells either are screened across zones of both manganese oxide (MnO_2) and iron-oxyhydroxide (FeOOH) reduction or, if irrigation wells with large abstractions, draw water from both paleochannel and interfluve because the command of the well is so large. For this study, we have not measured pH in groundwaters, but values reported elsewhere across JAM and the Bengal Basin are usually in the range 6.5 to 7.5 (e.g., *Stollenwerk et al.* [2007] and *McArthur et al.* [2004] for JAM data) and the similarity in composition across JAM suggests our new wells will have similar pH.

[34] The spatial distribution of the arsenic concentration in groundwaters is shown in Figure 8. Three zones are recognizable; the zonation bears little relation to the age of the aquifer sand but is correlated with sediment color i.e., is controlled by the sediment's content of FeOOH, as noted more locally by *McArthur et al.* [2004]. Beneath zone 1, which coincides with the LRZ and the inferred extent of the LGMP, aquifers of brown sand host groundwater with low concentrations of arsenic ($\leq$87 μg/L and mostly $\leq$30), >1 mg/L of manganese, and low amounts of dissolved iron (Figure 9 and Table 3). Beneath zone 2 and so outside the LRZ, sands are gray and the LGMP is absent; groundwater contains >87 μg/L of arsenic and generally much more,

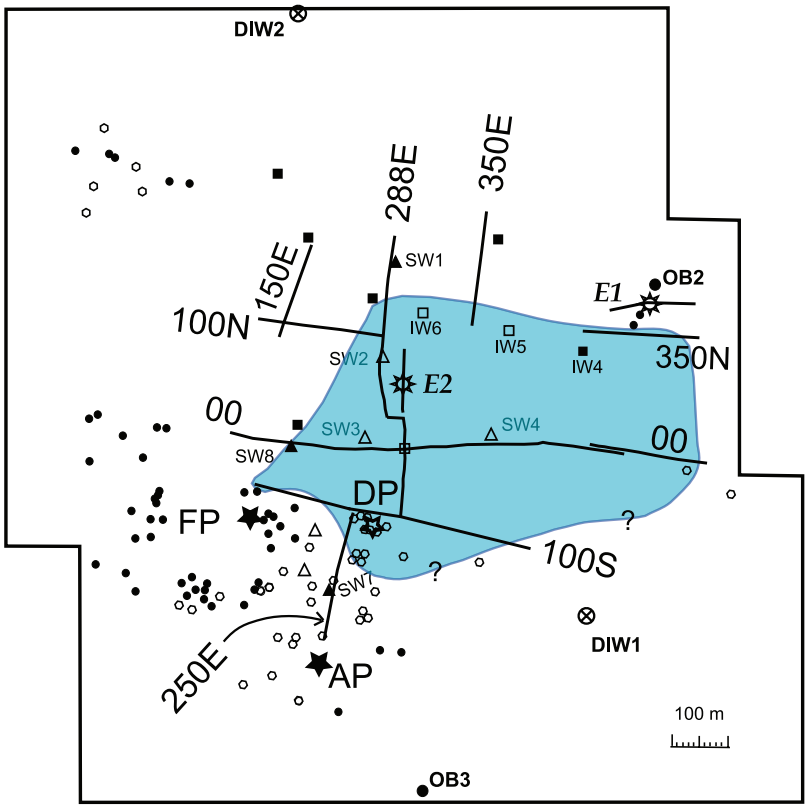

Figure 6. Survey lines for shallow resistivity. E1 and E2 are sites where expander arrays were run. A low-resistivity zone (LRZ) in the shallow subsurface lies beneath the colored area that occupies the central part of the study area and is interpreted to be the area beneath which lies a regional paleosol, the LGMP. The paleosol was proven by drilling at SW2, SW3, SW4, SW8 and DP. Beneath the paleosol, brown Pleistocene sands host low-arsenic water. Stars denote piezometers, squares denote irrigation wells, and triangles denote wells SW1–8 (see Figure 1 for numbering). Solid symbols are wells with >50 μg/L As; open symbols are those with <50 μg/L As.

little manganese, and mg/L quantities of dissolved iron. In zone 3, many wells tap As-free groundwater that is similar to that found in zone 1 because they are screened at the base of the aquifer, where a few meters of brown sand is present. Wells screened in the middle and upper parts of the aquifer in zone 3, however, sample groundwater from gray, reduced, sands and so are high in arsenic and iron, and low in manganese. For example, gray Pleistocene sands around

Table 1. Dates of Sediments From Sites AP, FP, and DP in the Study[a]

Site	Depth (m)	Sample Type	δ^{13}C (‰)	Year BP ± 1 Standard Deviation
		^{14}C Dates		
FP	7.6	organic-rich sediment	−18.1	2040 ± 100
FP	7.6	wood	−25.6	1945 ± 45
FP	29.2–29.9	organic-rich sediment	−28.6	7220 ± 40
FP (LAC)	49.5–50.4	dispersed OM in clay	−20.7	27230 ± 400 (U)
DP	5.2	organic-rich sediment	−22.9	1465 ± 105
DP	5.2	wood	−26.5	1155 ± 85
DP	15.2	organic-rich sediment	−27.7	7525 ± 95
DP	15.2	peat	−27.8	7350 ± 60
DP	16.8	wood	−27.9	7915 ± 75
		OSL Dates		
APOSL 1	10.0–10.5	quartz		3800 ± 1300
APOSL 2	19.0–19.5	quartz		7140 ± 490
APOSL 3	27.5–28.0	quartz		7640 ± 470
APOSL 4	31.0–31.5	quartz		6860 ± 570
APOSL 5	39.0–39.5	quartz		17500 ± 1160
APOSL 6	43.0–43.5	quartz		23400 ± 1460

[a]For the study area, see Figure 1. Dating was by optically stimulated luminescence on quartz from AP and by ^{14}C on organic-rich sediment, wood, and peat in a strict sense. FP (LAC) is a sample from the lower aquiclude at site FP; the age is a minimum (see text) and uncalibrated (U).

Table 2. Mean Chemical Composition of Sediments From the Study Area

Age	Lithostratigraphic Unit	Site	Number of Samples	Depth range (m)	Sample Type	SiO_2 (%)	Al_2O_3 (%)	Fe_2O_3 (%)	MnO (%)	CaO (%)	MgO (%)	Na_2O (%)	K_2O (%)	TiO_2 (%)	P_2O_5 (%)	TS (%)	TOC (%)	$CaCO_3$ (%)	As (ppm)	Ba (ppm)	Co (ppm)	Cr (ppm)	Cu (ppm)	Li (ppm)	Ni (ppm)	Sc (ppm)	Sr (ppm)	V (ppm)	Y (ppm)	Zn (ppm)
Holocene	Joypur Member	AP	21	12–30	gray sand	69.8	10.5	4.1	0.08	3.63	1.91	1.35	2.63	0.50	0.11	0.01	0.30	4.3	22	463	7.5	38	16	36	27	8.5	108	51	22	57
Holocene	Joypur Member	FP	11	13–29	gray sand	71.6	9.4	3.7	0.06	2.83	1.57	1.39	2.54	0.45	0.10	0.00	0.18	4.1	24	428	8.1	32	10	34	20	8.1	96	48	20	59
Pleistocene	LGMP Member	DP	3	21–23	LGMP[a]	46.7	21.4	10.5	0.13	0.80	1.39	0.28	2.95	1.01	0.11	0.00	0.19	0.2	146	897	19	169	39	5	##	25	50	118	73	106
Pleistocene	Moyna Member	DP	21	25–60	brown sand	82.3	7.7	1.8	0.03	0.67	0.40	1.14	2.13	0.21	0.04	0.01	0.09	0.1	11	386	1.6	14	8.1	17	15	4.5	68	22	14	28
Pleistocene	Ardevok Member	FP	11	30–47	gray sand, minor brown	81.9	7.6	2.0	0.05	1.23	0.56	1.23	2.12	0.23	0.06	0.01	0.13	1.3	9.1	380	3.2	15	3.1	16	9.5	4.5	76	25	15	45
Pleistocene	Ardevok Member	AP	2	39–44	gray + brown sand	81.1	7.1	1.8	0.05	1.65	0.70	1.34	2.01	0.26	0.06	0.01	0.11	1.5		335	4.4	23	8.0	18	10	4.3	76	26	13	28
Pleistocene	Sunti Clay Member	FP	5	48.0–48.6	brown weathered upper clay	54.8	14.1	6.6	0.07	5.10	2.91	0.77	3.21	0.52	0.10	0.00	0.25	8.1	62	541	12	60	37	54	38	14	102	75	23	84
Pleistocene	Sunti Clay Member	FP	14	49–70	green-gray unweathered clay	57.6	14.4	6.1	0.08	5.53	3.04	0.88	3.32	0.67	0.11	0.45	0.78	9.3	63	534	13	72	33	58	40	14	128	97	24	87
					Standard Deviations (1 SD)																									
Holocene		AP	21		gray sand	4.7	1.9	1.2	0.07	0.50	0.51	0.19	0.59	0.10	0.02	0.00	0.15	1.4	16	108	3.8	19	6.8	15	12	2.1	11	13	3.9	16
Holocene		FP	11		gray sand	2.4	0.9	0.8	0.01	0.45	0.37	0.07	0.28	0.09	0.01	0.01	0.06	1.0	14	45	2.4	12	4.4	9.1	6.5	1.4	6.3	12	3.2	16
Pleistocene		DP	3		LGMP	2.7	0.6	0.7	0.03	0.20	0.08	0.05	0.65	0.02	0.01		0.08	0.1	83	63	2.7	11	9.2	0.2	2.5	0.7	0.4	7.5	8.7	11
Pleistocene		DP	21		brown sand	2.2	0.9	0.5	0.02	0.24	0.13	0.18	0.28	0.05	0.01	0.00	0.02	0.2	4.9	58	1.1	6	2.8	10	7.0	1.3	9.2	5.7	3.7	6.3
Pleistocene		FP	11		gray sand, trace brown	2.2	0.4	0.5	0.03	0.56	0.16	0.14	0.15	0.06	0.02	0.01	0.05	0.7	1.9	40	1.2	5	2.0	3.2	3.8	1.4	4.2	4.9	6.2	22
Pleistocene		AP	2		gray + brown sand[b]																									
Pleistocene		FP	5		uppermost part, brown and weathered	2.9	0.5	1.2	0.01	1.11	0.17	0.08	0.09	0.14	0.02	0.0	0.10	1.5	17	45	1.6	6.3	7.3	3.9	2	0.8	6.9	20	2.1	5.5
Pleistocene		FP	14		green-gray unweathered clay	2.9	1.0	0.6	0.01	0.64	0.40	0.20	0.20	0.04	0.04	0.4	0.37	1.1	11	30	1.1	10	3.6	6.0	4	1.6	14	7.0	2.8	4.3

[a]For definition of the Last Glacial Maximum paleosol (LGMP), see text for explanation.
[b]Too few samples for reliable calculation.

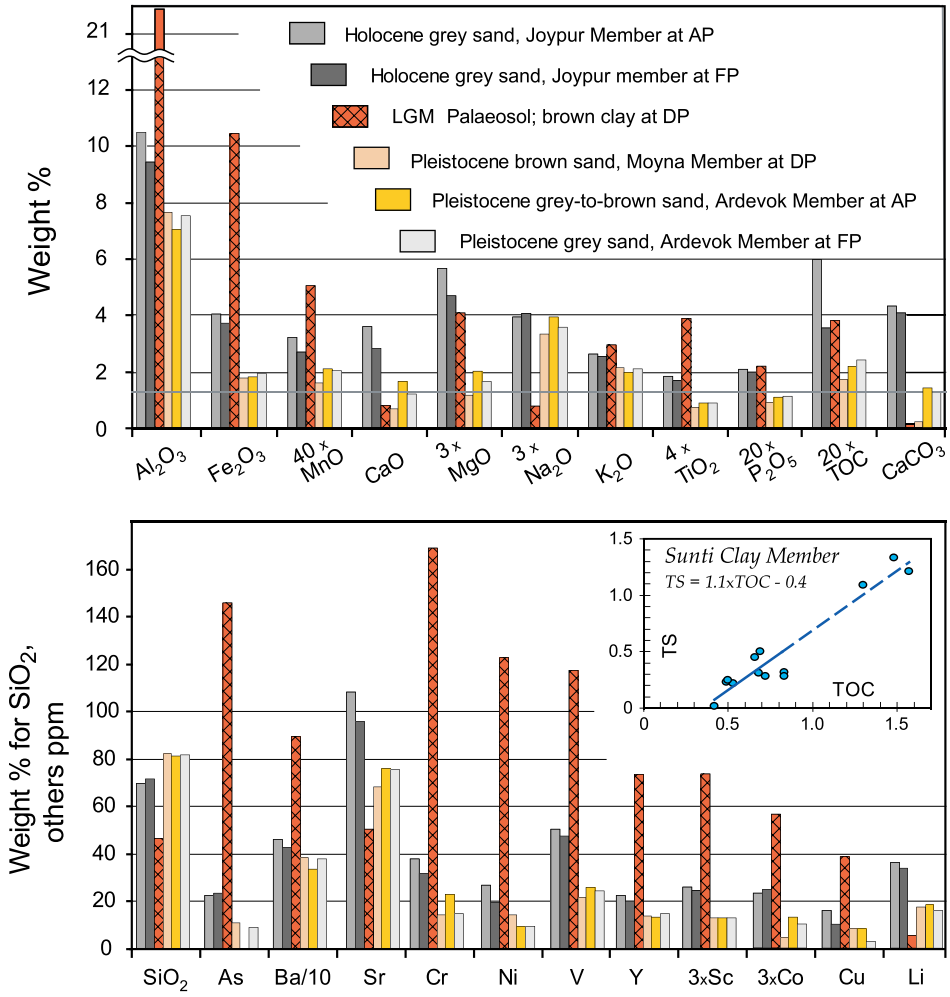

Figure 7. Graphical summary of the sediment composition given in Table 2. Inset shows C/S relation for the Sunti Clay Member (the lower aquiclude). The element abundances in the brown sands of the Moyna Member are close to those in the gray sands of the Ardevok Member. Both differ markedly from the element abundances in the Holocene gray sands of the Joypur Member. Compared to the Moyna Member, from which it is derived by weathering, the Last Glacial Maximum paleosol is enriched in immobile elements (e.g., Ni, Fe, Cr, V) and is depleted in mobile elements (Na, Li). Values plotted are means of between 2 and 21 analyses of individual lithostratigraphic units.

32 mbgl in AP yield groundwater containing >200 μg/L of arsenic, while brown Pleistocene sands at the base of the aquifer at AP yield water with <10 μg/L arsenic (Figure 9). Many of the inhabitants of zone 3 are aware of the good quality of water available in the brown sand locally present at the base of the aquifer. As a consequence, many have installed, or reinstalled, their well screens at that level, thereby giving the superficial impression that the region around AP (zone 3) is largely free of arsenic, when in reality, most of its shallow aquifer is As polluted.

[35] The low-As, Mn-rich groundwaters in brown sands, either of the Moyna Member in zone 1, or at the base of the Ardevok Member in zone 3, are at a different redox poise to the Fe and As-rich groundwaters found elsewhere. In the former, most groundwater is poised at the stage of MnO_2 reduction; if arsenic was originally sorbed on MnO_2 and was released by its reduction, that arsenic has been resorbed to unreduced MnO_2 or FeOOH [*Welch et al.*, 2000; *Stüben et al.*, 2003]. At the base and top of the aquifer in zone 1, iron concentrations are higher, and manganese concentrations lower, than they are centrally within the aquifer (Figure 9). A redox gradient thus exists, from MnO_2 reduction in the aquifer's center toward increasing (but minor) FeOOH reduction at its base and top. In contrast, in gray aquifer sands outside the LRZ, reduction of FeOOH is at an advanced stage, having progressed further along the redox gradient than in aquifers within the LRZ, although that reduction has not penetrated everywhere to the base of the aquifer (e.g., AP).

4.6. Piezometry

[36] Our measurements of water level are given in Table S2, and graphically in Figures 10, 11, and 12. In Figure 10a we show the distribution of leveled wells in which we measured water levels precisely in order to establish piezometric gradients and seasonal variations in water level. Wells labeled OB are in the far field, those labeled SW, and the piezometers AP, FP and DP, are in the near field.

Table 3. Location and Chemical Composition of Well Waters From the Study Area Analyzed for This Work

Well	°E	°N	Screen Depth (m)	As (μg/L)	Na (mg/L)	K (mg/L)	Ca (mg/L)	Mg (mg/L)	Sr (mg/L)	Ba (mg/L)	Fe (mg/L)	Mn (mg/L)	HCO_3[a] (mg/L)	Cl (mg/L)	SO_4 (mg/L)	F (mg/L)	PO_4 (mg/L)	H_4SiO_4 (mg/L)
DIW1[b]	88.49713	22.74037	175	2.7	57	4.6	87	24	0.54	0.16	0.8	0.1	522	12.2	2.6	0.2	0.1	72
DIW2	88.49174	22.75199	175	1.7	58	3.9	89	23	0.51	0.17	0.8	0.1	523	12.6	5.4	0.3	0.1	62
DTW1	88.49811	22.74588	176	1.8	63	5.1	100	27	0.58	0.19	1.4	0.2	593	11.6	2.5	0.3	0.5	65
DTW2	88.48385	22.74236	176	6.4	55	13.5	83	27	0.50	0.19	1.0	0.3	499	25.4	10.7	0.9	4.7	63
SW1	88.49328	22.74666	41	299	75	3.5	128	42	0.75	0.19	7.2	0.2	765	31.1	2.2	0.2	1.9	50
SW2	88.49303	22.74489	37	30	107	1.4	116	33	0.60	0.17	2.0	2.2	781	16.7	3.4	0.5	1.1	49
SW3	88.49272	22.74328	36	1.5	52	1.2	154	31	0.56	0.09	0.3	3.0	671	58.8	1.1	0.4	0.3	56
SW4	88.49507	22.74333	36	1.0	44	1.0	119	24	0.40	0.11	0.3	2.9	580	14.9	0.6	0.2	0.4	56
SW5[c]	88.49167	22.74167	50															
SW6	88.49163	22.74073	46	<10	30	2.3	133	38	0.54	0.05	1.1	1.9	569	59.6	10.1	0.3	0.3	59
SW7[d]	88.49205	22.74050	46	150														
SW8	88.49136	22.74312	41	1410	48	3.2	125	39	0.70	0.07	9.0	0.1	633	57.1	0.3			
IW2	88.49345	22.74305	40	<1	58	0.9	135	25	0.45	0.11	0.1	3.1	632	38.7	0.1	0.5	0.4	56
IW3	88.49146	22.74355	30	578	71	2.7	127	38	0.65	0.14	8.3	0.3	702	48.6	0.9	0.1	2.1	49
IW4	88.49678	22.74495	34	87	68	1.8	116	29	0.45	0.28	9.5	1.0	689	9.2	0.1	0.3	3.7	51
IW5	88.49535	22.74536	34	49	59	1.2	130	31	0.57	0.30	10.8	1.9	720	11.0	0.0	0.3	3.0	55
IW6	88.49379	22.74571	26	28	73	1.1	127	31	0.53	0.33	8.4	1.7	732	15.1	0.0	0.3	3.1	53
IW7	88.49282	22.74595	40	251	99	3.2	120	40	0.79	0.14	7.9	0.2	787	38.7	0.0	0.1	2.1	54
IW8	88.49165	22.74716	30	569	37	2.9	128	34	0.50	0.44	7.2	0.2	662	9.8	1.0	0.2	3.3	56
IW9	88.49110	22.74838	40	169	23	2.3	93	23	0.33	0.25	8.1	0.2	463	10.6	0.7	0.2	3.0	56
IW10	88.49515	22.74711	30	58	66	2.5	129	31	0.49	0.31	10.8	0.4	732	11.1	0.0	0.3	3.7	56
OB 1[e]	88.48407	22.74307	34															
OB 2[e]	88.49790	22.74632	40															
OB 3[e]	88.49387	22.73685	51															
OB 4[e]	88.49485	22.76081	40															

[a]Calculated by difference using Cl and SO_4 only.
[b]Central Ground Water Board well 176-T, installed in 1970.
[c]Lithology only recorded. No pipe installed.
[d]Field test for As; no other analysis done.
[e]Location, depth, and water level data only; see Table S2.

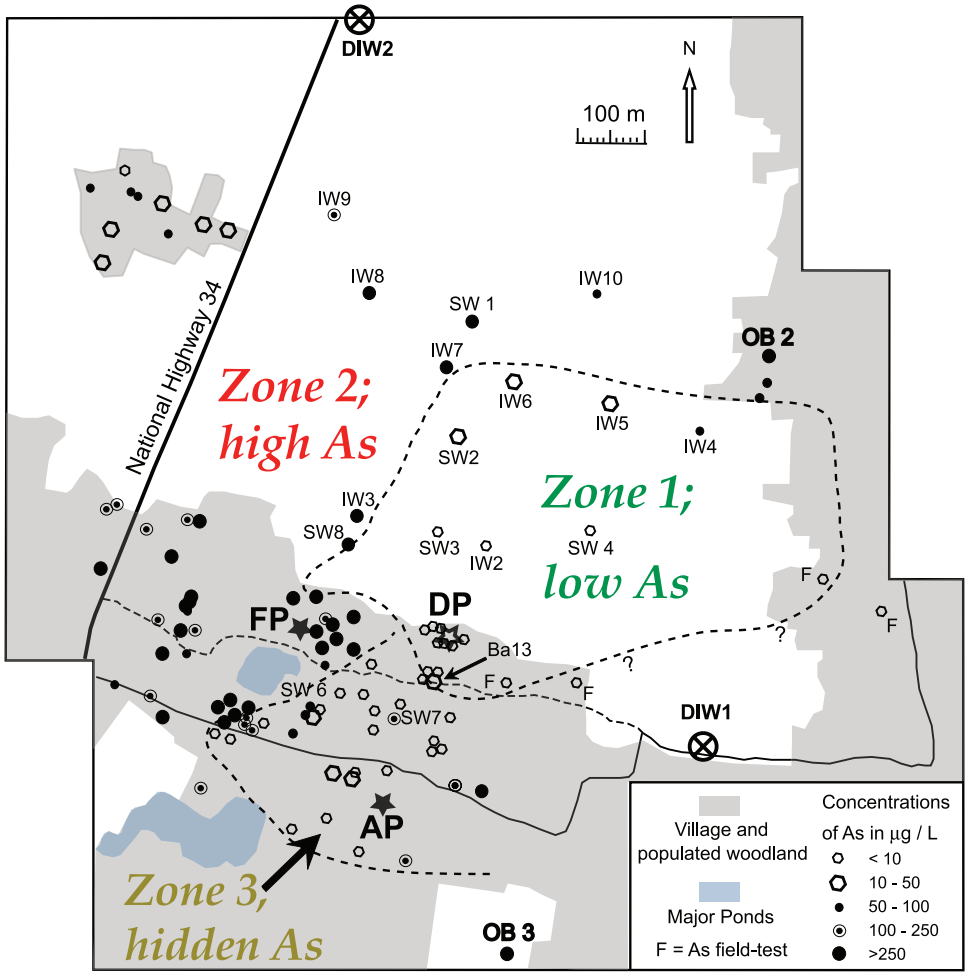

Figure 8. Geographical variation of arsenic concentration in the shallow aquifer across the study area. Zone 1, which coincides with the LRZ and the LGMP, yields low-As groundwater from brown sands poised at manganese reduction. Zone 2, which is outside the LRZ and where the LGMP is absent, yields As-polluted groundwater in aquifers undergoing FeOOH reduction. In zone 3 most of the aquifer thickness is As polluted and iron rich, but a basal few meters are brown sand poised at manganese reduction and yielding low-As groundwater. The basal brown sand in zone 3 is a target for installing (temporarily) safe wells, so zone 3 appears to be low in As, while in reality it is polluted.

Figure 10b shows piezometric profiles of water in the upper aquitard and the shallow aquifer as a function of depth. Figure 10c shows depth to midscreen in the piezometers and monitoring wells plotted against piezometric level, to demonstrate that horizontal hydraulic gradients within the shallow aquifer are insensitive to screen depth. In Figure 11 we show seasonal fluctuations of water level over 2 years in wells in the shallow aquifer (Moyna Member, Joypur Member, Ardevok Member) along a N–S transect from AP in the south to SW1 in the middle of JAM, a distance of around 700 m (Figures 1 and 10). Water levels fluctuated seasonally and in phase at all sites, with an annual range of about 4 m. Similar fluctuations are seen in the upper aquitard (Hoogli Member), but are not shown for reasons of brevity (see instead Table S2).

[37] Horizontal flow in the upper aquitard (Figure 12), at 10 mbgl, is to the south in the southern part of JAM (north of DP), where it is driven by a water table mound in the thick, peaty silts that overlie the impermeable LGMP. Horizontal flow at depths of 25 to 48 m in the shallow aquifer (Figure 12) is to the north-northeast, driven by horizontal gradients of around 0.0009. The typical intergranular velocity of groundwater flow is therefore around 0.1 m/d (30 m/a). The hydraulic gradients vary seasonally, as can be seen from the seasonal compression and expansion of water level along the 700 m profile from AP to SW1 that is shown in Figure 11. Horizontal gradients were high (greater data spread) at the height of the monsoon (July and August) and during high abstraction for irrigation in the dry season, e.g., the measurements for 2006, which were made after irrigation for a new rice crop had largely completed (see Table S2). The maximum horizontal gradient recorded was 0.0015.

[38] Throughout the year, and at all piezometers, downward hydraulic gradients exist between the upper aquitard and underlying aquifer (Figure 10b); the head difference is greatest where the LGMP confines the underlying Moyna Member, and a maximum of 3.7 m was recorded at DP. At

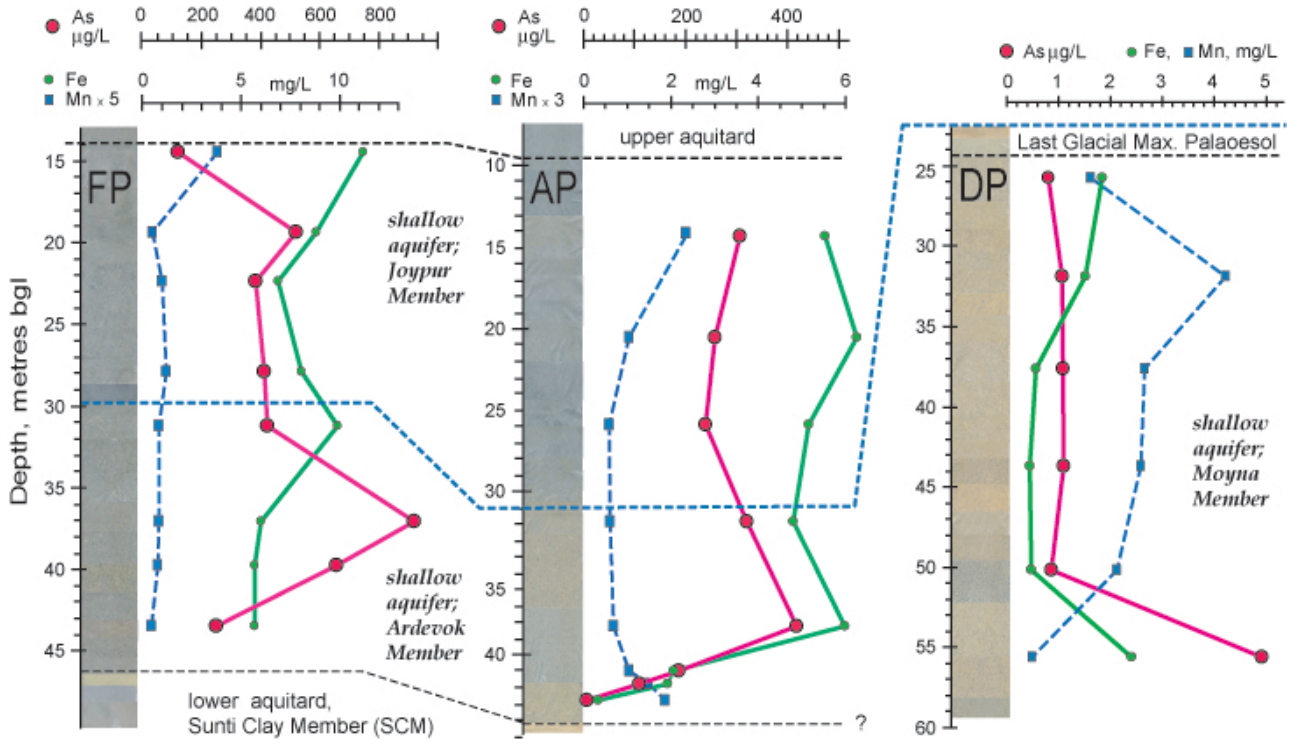

Figure 9. Vertical profile of Fe, Mn, and As concentrations in groundwater from piezometers FP, AP, and DP; see Figure 1 for locations (data from *McArthur et al.* [2004], reproduced in Table S1). In DP, the redox status of groundwater, defined by Fe and Mn concentrations, is poised at MnO_2 reduction in its center, with a tendency toward FeOOH reduction above and below. At AP, only the lowermost part of the aquifer remains at MnO_2 reduction; higher levels have progressed to FeOOH reduction, releasing significant amounts of arsenic to groundwater.

AP and FP, where the LGMP is absent, the aquifer is semiconfined and the head difference was typically 0.3–1.0 m. In the upper part of the aquifer a small downward hydraulic gradient existed throughout the year: at AP, DP, and FP respectively, mean downward gradients over the 2-year period of monitoring in the upper part of the aquifer were 0.0060, 0.0009, and 0.0005, with respective uncertainties (1 standard deviation) of ±0.0018, ±0.0006, and ±0.0003 quantifying the seasonal variation (see Table S2). Over the lower part of the aquifer, average gradients were indistinguishable from zero. Assuming an isotropic aquifer, these results convert to vertical flow velocities in the upper part of the aquifer of 0.6 m/d at AP, 0.1 m/d at DP and 0.05 m/d at FP. However, some vertical anisotropy is likely, in which case the vertical flow rates would be slower. These measurements show that horizontal and vertical rates of groundwater flow are of a similar order of magnitude in the upper part of the shallow aquifer.

4.7. Hydraulic Properties

[39] The results of the slug tests are summarized in Figure 13. Slug tests on sands gave overdamped responses, and yielded permeabilities of between 12 and 50 m/d, with an average of 30 m/d. These values are typical of medium to fine sands in the Bengal Basin, but the difference between the average hydraulic conductivity of gray sands (34 m/d) and brown sands (28 m/d) in our study area is much smaller than differences between gray and brown sands in Bangladesh [*Ravenscroft*, 2003]. At AP, SW1, SW5, and SW7, the sands of the Joypur Member and the sands of the underlying Ardevok Member appear to be hydraulically connected. Slug tests on piezometers screened in the Hoogli Member (the upper aquitard) at DP and FP, showed underdamped responses, and gave permeabilities of 0.011 and 0.061 m/d respectively. Interpretation of the slug test at AP was complicated by a partial connection of the well screen with the underlying aquifer, so the result overestimates the permeability of the Hoogli Member.

[40] The results of the pumping tests are summarized in Figure 13. During pumping tests at AP8, FP6, and DP1, drawdowns of a few centimeters were observed at all depths in the shallow aquifer in the first few minutes. There was little difference in the magnitude or timing at different depths, an observation that indicates good vertical hydraulic continuity. Drawdowns were too small to be effectively separated from barometric fluctuations after as short a period as 10 min. Because only a small proportion (around 5%) of the aquifer was screened by the pumping well, reliable estimates of transmissivity could not be obtained, but the results suggest values of several hundred m^2/d. Better estimates of transmissivity of the shallow aquifer, of between 940 and 1140 m^2/d, were obtained by combining lithology and slug test results.

[41] Monitoring of water levels in the Hoogli Member (the upper aquitard) at AP and FP during pumping of the aquifer beneath showed weak and delayed responses; measurements were complicated by barometric effects and are

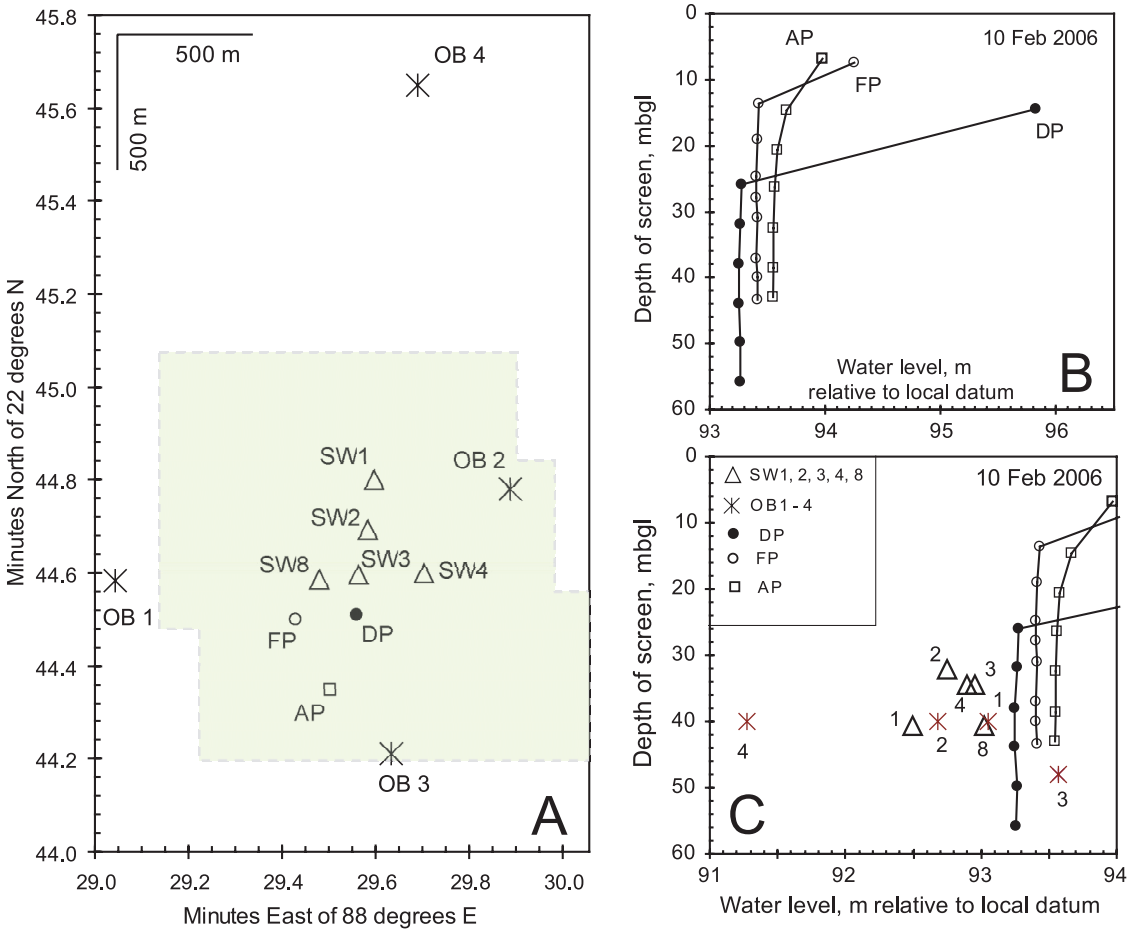

Figure 10. (a) Piezometer distribution in JAM. Shaded irregular box is the area of the map shown in Figure 1. (b) Water levels on 10 February 2006, relative to an arbitrary datum set at 100 m at piezometer AP; the shallowest well at each piezometer site is screened within the upper aquitard (Hoogli Member of the Joypur Alluvium) and has exceptionally high levels. (c) Cross plot of screen depth in observation wells against water level in the wells on 10 February 2006. The plots show the pronounced vertical hydraulic gradient at piezometer AP and the fact that the horizontal piezometric gradient is insensitive to screen depth. Comparison with spot heights on Survey of India topographic sheets suggests a ground elevation of 7–8 m amsl. Water levels in all ponds are above contemporaneous groundwater levels.

not suitable for quantitative analysis. The low permeability of the LGMP was demonstrated by the hydraulic response at DP. Water pumped from 50 m produced an almost immediate response at 25 m (in DP7) but produced no drawdown in the upper aquitard (DP2).

[42] The pumping test at DP demonstrated the vertically heterogeneous permeability of the Hoogli Member (the upper aquitard). Within 15 min of the discharge of pumped water to the surface, a rise in water level was seen in the piezometer screened in the upper aquitard at 15 mbgl. This observation showed that the water had infiltrated to the water table at 3 mbgl. Thereafter, the water table in the Hoogli Member rose steadily until about 15 min after pumping stopped, after which it remained stable for the next 60 min at a level 50 cm higher than before pumping. The rise produced no detectable response in piezometer DP7 that was screened only one meter below the LGMP. Thus we conclude that the upper part of the Hoogli Member (the upper aquitard) has significant vertical permeability, but the underlying LGMP is effectively impermeable.

4.8. Abstraction

[43] We estimate an annual abstraction for irrigation of 230,000 m^3 from the shallow aquifer and 270,000 m^3 from the deep aquifer. The figures are derived by mapping the geographical areas in JAM commanded by shallow and deep irrigation wells, and assuming a crop water requirement for irrigation of 500 mm/a [*Ravenscroft*, 2003] and a deep percolation loss of 33%. Domestic withdrawals are estimated at 17,000 and 3,600 m^3 respectively, assuming 10 users per well in the shallow aquifer, each using 20 L/d, and 20 users per well using the 20 L/d from each deep well. The total abstraction is thus 247,000 plus 274,000 m^3, respectively.

5. Discussion

5.1. Evolution of the Bengal Basin

[44] To set the interpretation of our study area into its regional context, we first outline the evolution of the Bengal Basin during the Pleistocene and Holocene, and then show how this evolution relates to the hydrogeology of our area.

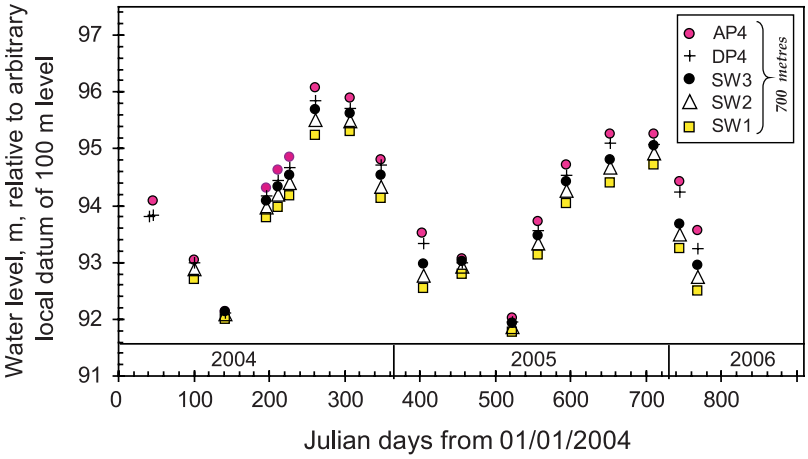

Figure 11. Seasonal variation of water level in wells spaced along a 700 m, N–S traverse from AP in the south to SW1 in the north (Figures 1 and 10). Elevations are relative to an arbitrary site datum at piezometer AP that was set to 100 m elevation. Absolute heights relative to sea level are unknown, but comparison to topographic maps suggests that the area is at an elevation of 7–8 m above mean sea level. Note that the horizontal hydraulic gradient, shown by the data spread along the profile, varies with the season and is greatest in February, around the time wells are pumped to irrigate the dry season rice crop, and least in the wet season as aquifers fill.

At the time of the Last Glacial Maximum (LGM) at around 20 ka, sea level was some 120 m lower than now [*Lambeck et al.*, 2002]. Erosion between 125 ka and 20 ka had created a broad coastal platform formed of interfluves (Figure 14) at an elevation 20–50 m below the present land surface, around upstanding blocks (e.g., Madhupur and Barind tracts) that had been bypassed by river erosion up to that time [*Bangladesh Agricultural Development Corporation and Overseas Development Administration (BADC)*, 1992; *Umitsu*, 1993; *Goodbred and Kuehl*, 2000a, 2000b; *Goodbred et al.*, 2003]. The paleosurface was incised to at least base level (120 mbsl) along major river channels, and less deeply along tributaries (Figure 15). The interfluves were weathered and oxidized to depths of tens of meters. We suggest that this alteration formed a basin-wide paleosol that is represented in our area by the LGMP that underlies some of our study area. It is important to note that this paleosol surface is not the same weathering surface that currently caps the Barind and Madhupur tracts, which have a far more complex history than does the LGMP.

[45] Sea level rose rapidly between 18 and 11 ka forming estuaries, along the incised rivers, that were subsequently infilled mainly by sand. Such deposition of sand in incised Pleistocene channels is well known in Bangladesh [*Umitsu*, 1993; *Ravenscroft*, 2003] and elsewhere [e.g., *Schumm*, 1993; *Blum and Törnqvist*, 2000 and references therein]. Between 12 and 10 ka, rising sea level inundated the interfluvial platform [*Kudrass et al.*, 1999; *Goodbred and Kuehl*, 2000a, 2000b; *Allison et al.*, 2003], allowing sediment to be deposited widely across interfluvial platforms. The sediment supply increased as Himalayan glaciers retreated, and monsoonal conditions intensified from the early Holocene to the climatic optimum at 8 ka, when rainfall, temperature and river flow were much higher than now [*Goodbred and Kuehl*, 1999; *Sharma et al.*, 2004]. This strong pulse of increased water and sediment supply between 10 and 8 ka [*Goodbred and Kuehl*, 2000a] rejuvenated local rivers and pushed the coastline south. Extensive peat basins developed [*Brammer*, 1996; *Islam*, 2001, *Ravenscroft et al.*, 2001], but were buried or displaced southward by later delta progradation after the rate of rise in sea level slowed around 6 ka.

[46] The essentials of this regional picture that are crucial to the interpretation of our area are that (1) the LGMP is a key stratigraphic marker; (2) it formed basin wide, albeit discontinuously; (3) it forms a regional, but discontinuous, aquitard that is preserved in interfluvial areas of the Bengal Basin; and (4) Holocene sands, both estuarine and fluvial, infill paleoriver channels where the LGMP was eroded by rivers or never deposited.

5.2. Application of the Regional Model to the Study Area

[47] The regional model envisages the LGM as a time when river channels were incised deeply into the eroded and weathered interfluvial surface. The range in size would have been similar to today; from those made by large regional rivers to those formed by small local tributaries (Figure 15). The main channels would have incised to a depth in equilibrium with sea level. Smaller tributaries, originating on the interfluves, may have been seasonal, and would have had beds perched above both sea level and the regional water table. It is the second type that is represented in our study area.

[48] Applied to JAM, this regional model suggests that the two sedimentary sequences we have identified represent a (tributary) paleochannel sequence and a paleointerfluve sequence. The paleochannel sequence is exemplified by the sediment profiles at FP, AP, SW1, SW5 and SW7. It comprises Holocene sand (Joypur Member) over reworked Pleistocene sand (Ardevok Member) in good vertical hydraulic connectivity. The paleointerfluve sequence is exemplified by the profiles at DP, SW2, SW3, SW4, SW6 and SW8 (Figure 4). It comprises the brown, oxidized, weathered brown sands of the Moyna Member beneath the

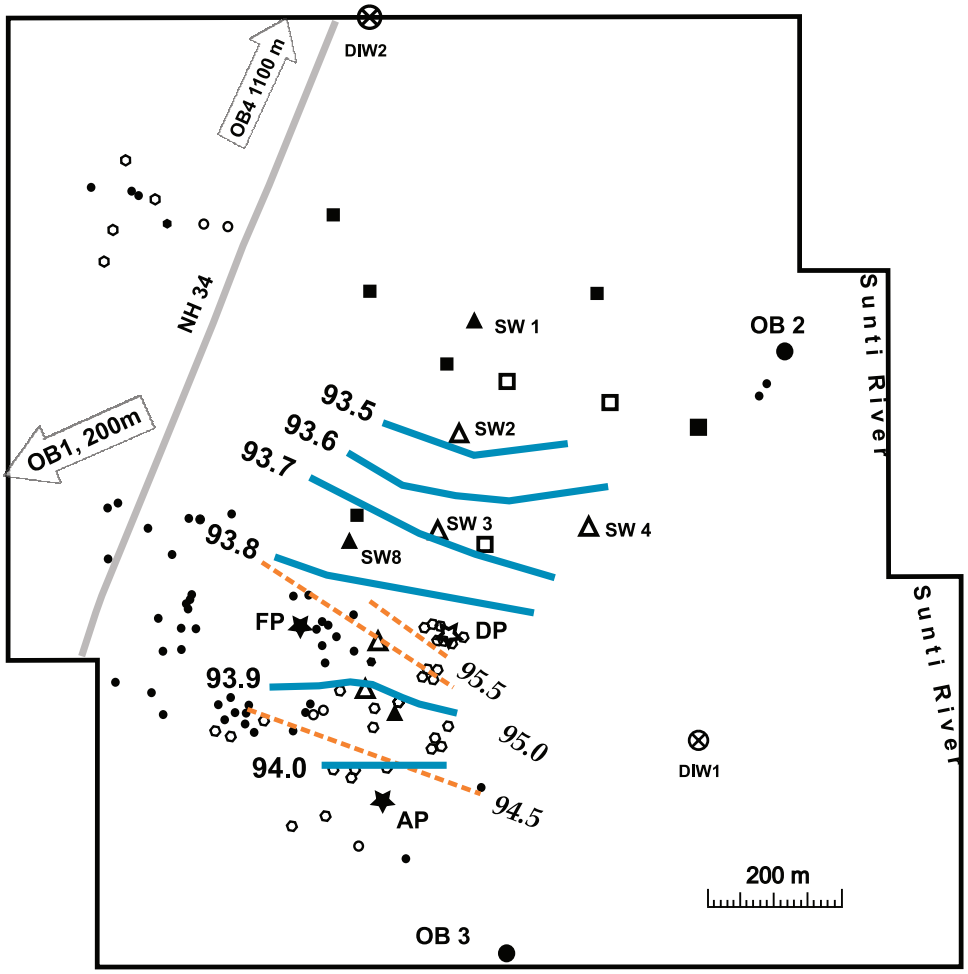

Figure 12. Piezometric contours across the study area for the shallow aquifer (solid blue lines) and for the upper aquitard (dashed orange lines) in February 2004. In the shallow aquifer, flow is to the north-northeast. In the upper aquitard, water mounds above the impermeable paleosol (LGMP) at 24 mbgl, and flow off the mound is captured in JAM as a southerly flow. Data used are water levels in AP, DP, FP, SW1, SW2, SW3, SW4, and SW8. Repetitive measurements of water level and inclusion of water levels in far-field observation wells OB1–4, confirm the direction of flow (see water level data in Table S1). Comparison with spot heights on Survey of India topographic sheets suggests a ground elevation of 7–8 m amsl.

LGMP. Because they are capped by the LGMP, the brown sands of the Moyna Member are hydraulically separated from overlying Holocene silts (Hoogli Member). The brown sands are, however, in lateral hydraulic continuity with the Ardevok Member, and so also, via that unit, to Holocene sands of the Joypur Member. We represent this interpretation in Figure 16 and justify it below.

[49] At the base of the sequence is the Sunti Clay Member. The radiocarbon dating for this unit is 27.2 ka (Table 2), a date we consider to be a minimum (see section 4). The top of this unit is now at an elevation of around −40 m, relative to sea level. Rejecting major uplift, the most recent time at which sea level was high enough to deposit the unit was prior to about 50 ka [*Lambeck et al.*, 2002], so we take the real age to be late Middle Pleistocene. That the upper few decimeters of this unit are brown, oxidized, and low in TOC and TS, supports the interpretation of an older age because weathering would have occurred when sea level was below −40 m between 50 ka and about 10 ka. Pleistocene sand of the Barasat Formation overlies the Sunti Clay. The LGMP caps the Moyna Member and represents a period of weathering and exposure that must have occurred after deposition of that member and before it was submerged by rising sea level after the LGM. Thus, the brown sands of the Moyna Member and the LGMP represent an old landscape, now buried but dissected when exposed, that was weathered prior to the post-LGM transgression (Figures 14 and 15).

[50] The Pleistocene sands of the Ardevok Member, and the Holocene sands of the Joypur Member, fill paleochannels that were incised through the paleosol-capped coastal plain during the Pleistocene and, in places such as at DP, into the Sunti Clay Member. The paleochannel fill developed in two stages: first, the brown sand of the Moyna Member was reworked locally in the terminal Pleistocene (24–18 ka; Table 1 and Figures 4 and 14–16) and redeposited as the Ardevok Member. The similarity in chemical composition attest to the commonality of these two mem-

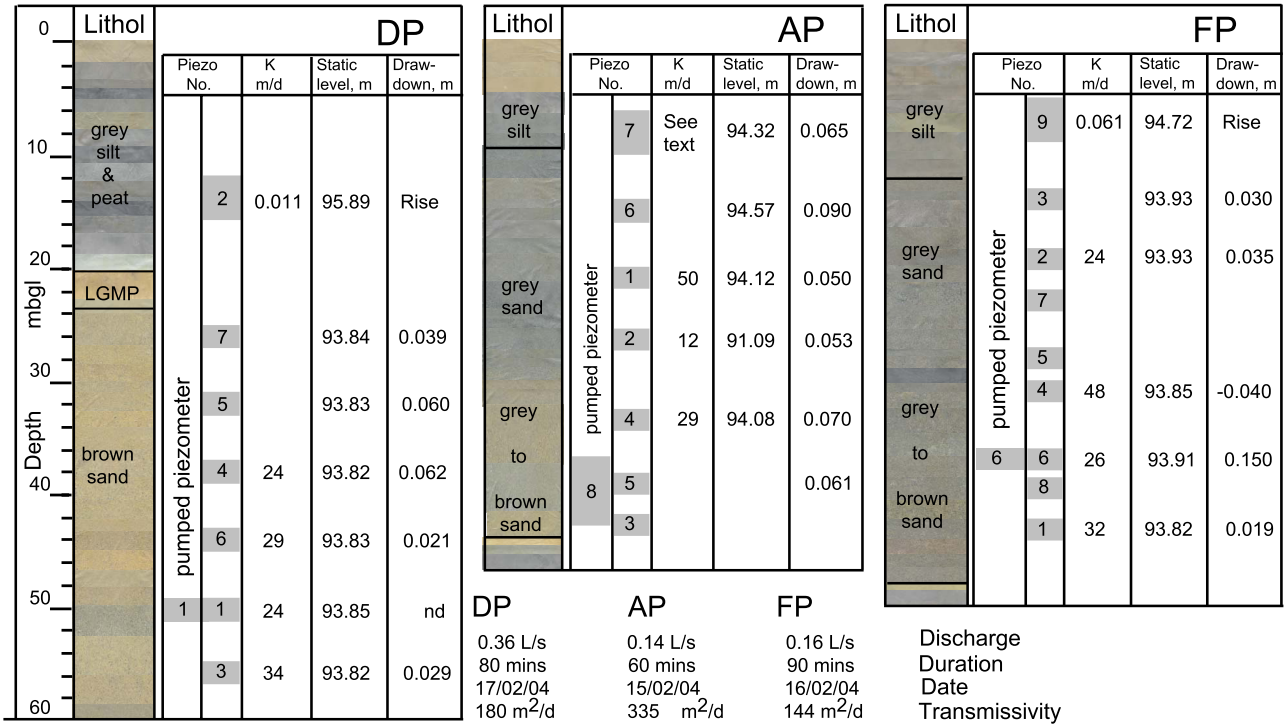

Figure 13. Summary of hydraulic testing at the AP, DP, and FP piezometer nests. The static water levels are elevations measured on 17 February 2004 relative to arbitrary site datum of 100 m. Static water level and drawdown are in meters. The transmissivity estimates are derived from pumping tests, and the hydraulic conductivity (K) estimates are derived from slug tests. In our modeling (Figure 19 and text) we prefer to use transmissivity values derived from lithology and slug tests.

bers (Figure 7). Second, rapid aggradation of fluvial gray sands occurred in the early Holocene when rising sea level forced an accompanying rise in the region's water table. The rise in sea level was accompanied by a landward shift in the focus of sediment deposition [*Goodbred and Kuehl*, 1999], filling the paleovalleys and their tributaries.

[51] After 7 ka in southern West Bengal, the depositional environment was that of a floodplain (Figures 14 and 15). Organic-rich sediment and peat accumulated widely across the Bengal Basin between 7–8 ka and 5–6 ka [*Islam and Tooley*, 1999; *Goodbred and Kuehl*, 2000a; *Goodbred et al.*, 2003], and around Kolkata between 6.5 to 2.0 ka [*Banerjee and Sen*, 1987]. This phase of development saw deposition of the Hoogli Member of the Joypur Alluvium. Layers of peat, in the strict sense, exist in the unit at DP, SW2, SW3, SW8, with less abundant plant remains at SW4 (Figure 17). This abundance is reflected in the composition of the Hoogli Member silts (Figure 17 and Data Set S1), which shows high TOC at these sites (up to 34% at 16.8 m in DP), and numerous values over 1% elsewhere except at SW7 where the maximum is 0.7%.

[52] In summary, the sedimentary sequence for the shallow aquifer may be described in terms of two sequences, i.e., paleointerfluve and paleochannel (Figures 4 and 14–16). The shallow aquifer is laterally extensive and is strongly confined in the paleointerfluvial areas overlain by the LGMP i.e., beneath the LRZ. Elsewhere, paleochannels juxtapose stacked Holocene and Pleistocene sands in good vertical hydraulic continuity. The upper aquitard (i.e., the Hoogli Member) that overlies the whole area is a semi-confining horizon that permits some flow, at least in its upper part.

[53] Hydraulic testing at the DP piezometer nest confirmed that the LGMP is effectively impermeable. We postulate that it forms a regional, if discontinuous, aquiclude, with uniform properties and geophysical expression across the Bengal Basin. In other areas, rather than the LGMP being overlain by organic-rich silts, as it is in our area, it may be that sands equivalent to the Joypur Member may commonly overlie the LGMP, giving rise to polluted aquifers that overlie unpolluted aquifers, but without hydraulic connection (as at Matlab [*von Brömssen et al.*, 2007]). This circumstance emphasizes the hydraulic control exerted on groundwater flow by the impermeable LGMP, and we examined this next. While other impermeable horizons undoubtedly exist in the subsurface of the Bengal Basin, three things set the LGMP apart from other impermeable horizons: its scale and putative lateral continuity, its uniform character, the fact that it caps (physically sits upon) the underlying unpolluted sands.

5.3. Conceptual Model of Flow

[54] Groundwater in JAM moves north-northeast from a region that is polluted by arsenic into a region that is currently unpolluted by arsenic because it is confined by the impermeable LGMP. A conceptualization of that flow is essential to understanding the distribution and movement of both water and arsenic in the region, and is given

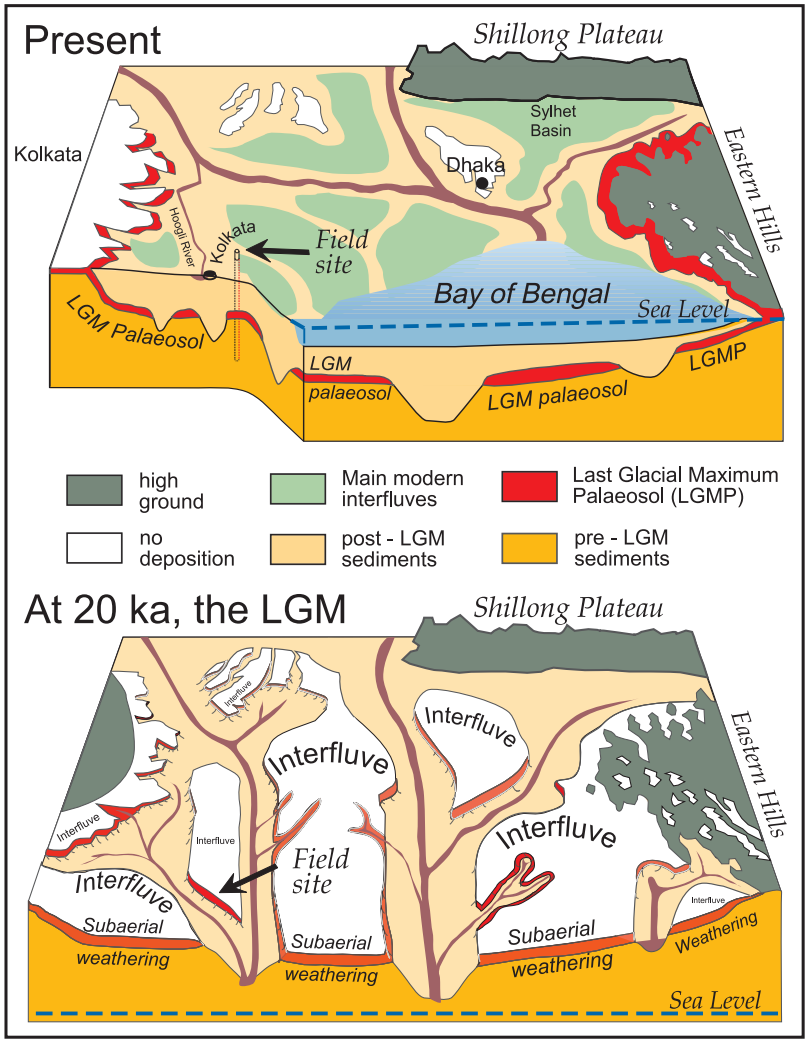

Figure 14. Outline evolution of the Bengal Basin's sedimentary architecture [after *Umitsu*, 1993]. At 20 ka, the lowstand of sea level at the Last Glacial Maximum causes deep erosion in paleochannels. Higher gradients than in the present caused the rivers to flow more directly south than they do today. Interfluvial areas were deeply weathered by the high rainfall and developed a widespread paleosol of impermeable clay that is found widely today across the Bengal Basin. The size of paleointerfluves shown is indicative only and is not meant to accurately indicate their possible current extent; we have not, for example, shown the numerous incising tributaries that must have been present at 20 ka.

in Figure 18. Following the conceptualization, we model the flow using the code MODFLOW [*Harbaugh et al.*, 2000] and present the result in Figure 19.

[55] The shallow aquifer in JAM is recharged by rainfall during the monsoon, and by irrigation water during the dry season in the cultivated fields in central and northern JAM. Recharge from ponds is negligible [*Sengupta et al.*, 2008]. Above the impermeable LGMP, recharge creates a groundwater mound in the upper aquitard. As a consequence, water flows laterally through the upper aquitard to regions where the LGMP is absent, then vertically down to recharge the shallow aquifer. The horizontal hydraulic gradient in the upper aquitard is approximately 0.01, which could equate to a flow velocity of up to 1 m/a. This flow is significant because about 55% of the irrigation water is drawn from the deep aquifer (section 4.8), but all excess irrigation water recharges the shallow aquifer. This flow through the upper aquitard is also important because it occurs through organic-rich sediment (Data Set S1), so water recharged through it will be anoxic and acquire small organic moieties from the anoxic fermentation of organic matter. These moieties will drive reduction of MnO_2 and FeOOH [*Ravenscroft et al.*, 2001] both in the upper aquitard and in the aquifer sands. This upper aquitard is the only source of organic matter available; soils in JAM are organic poor and, even were they not, little organic matter would escape the soil zone.

[56] In response to recharge and abstraction, groundwater flow in the shallow aquifer (but not the upper aquitard) in JAM is to the north-northeast at all depths. We show this conceptually in Figure 18 along a cross section running S–N through our area. The ends of the traverse represent Holocene channel fill, e.g., at AP and SW1, where the upper aquitard allows most recharge (Figure 10b). The middle part of the section represents the paleointerfluve sequence below the LRZ that is typified by the sequence at DP, SW3, SW2

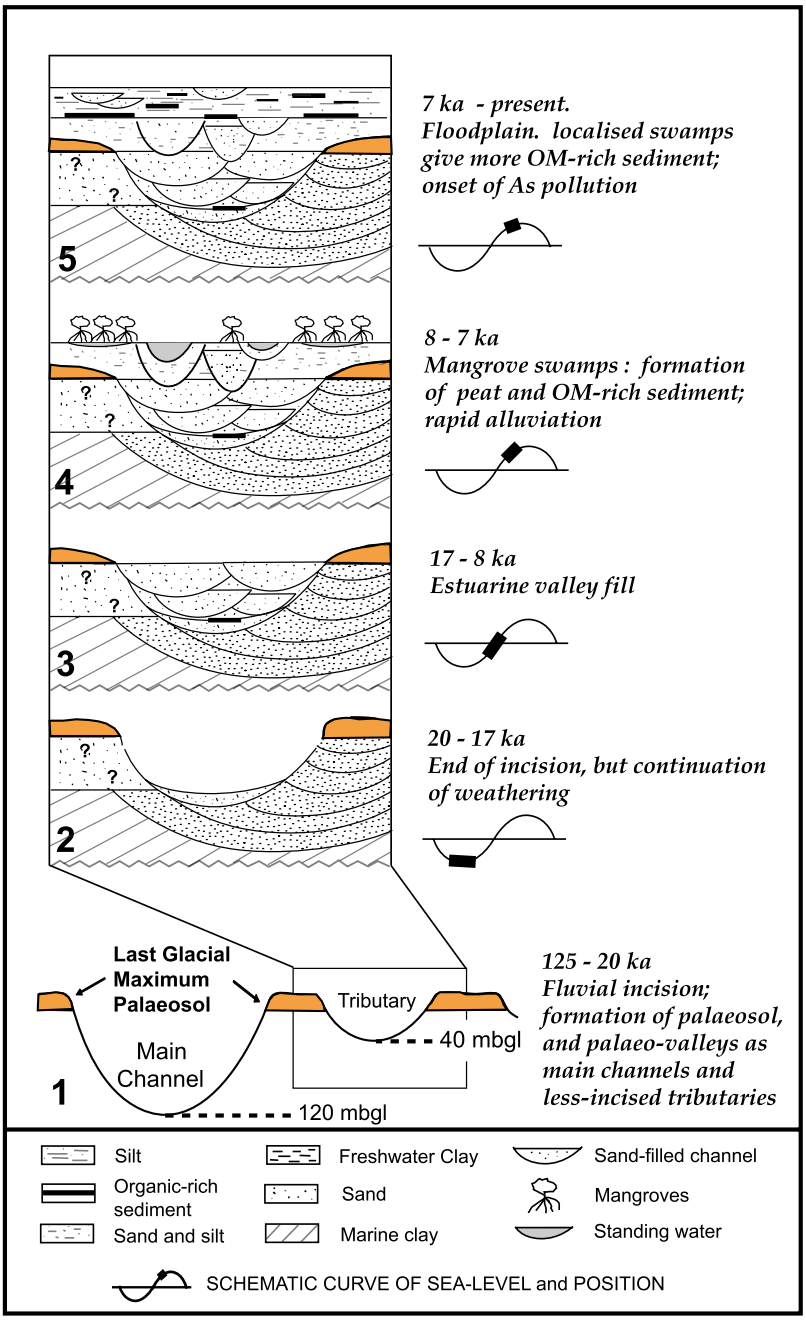

Figure 15. Generalized evolution of the Bengal Basin's sedimentary architecture, based on *BADC* [1992], *Umitsu* [1993], *Goodbred and Kuehl* [2000b], and *Goodbred et al.* [2003]. The insets illustrate stages of erosion and valley incision consequent on falling sea level (inset 1), weathering (inset 2), valley fill (inset 3), mangrove development (inset 4), and floodplain deposition (inset 5). The onset of pollution is presumed to have started around 2 ka when deposition of the upper aquitard (see Table 1 and Figure 16) confined the units below and allowed anoxic conditions to become established.

and SW4, where the impermeable LGMP prevents recharge to the aquifer.

[57] Flow through the confined Pleistocene sand (Moyna Member) under the LGMP approximates a one-dimensional flow path. Using the transmissivity estimate for the DP site of 944 m^2/d, and hydraulic gradient (Figures 10 and 11) of 0.0009, the discharge per meter width is 0.66 m^3/d. Thus, assuming a porosity of 0.3, and homogenous distribution of permeability, a horizontal flow velocity of 30 m/a is estimated. Inhomogeneity certainly will exist in the subsurface, but its quantification is typically not possible in hydrogeological studies because of constraints of cost and time.

[58] Flow is moving arsenic-polluted groundwater from paleochannel regions undergoing FeOOH reduction into unpolluted paleointerfluvial regions containing low-As water. The rate at which arsenic moves will be less than the rate of groundwater flow, owing to adsorption of arsenic

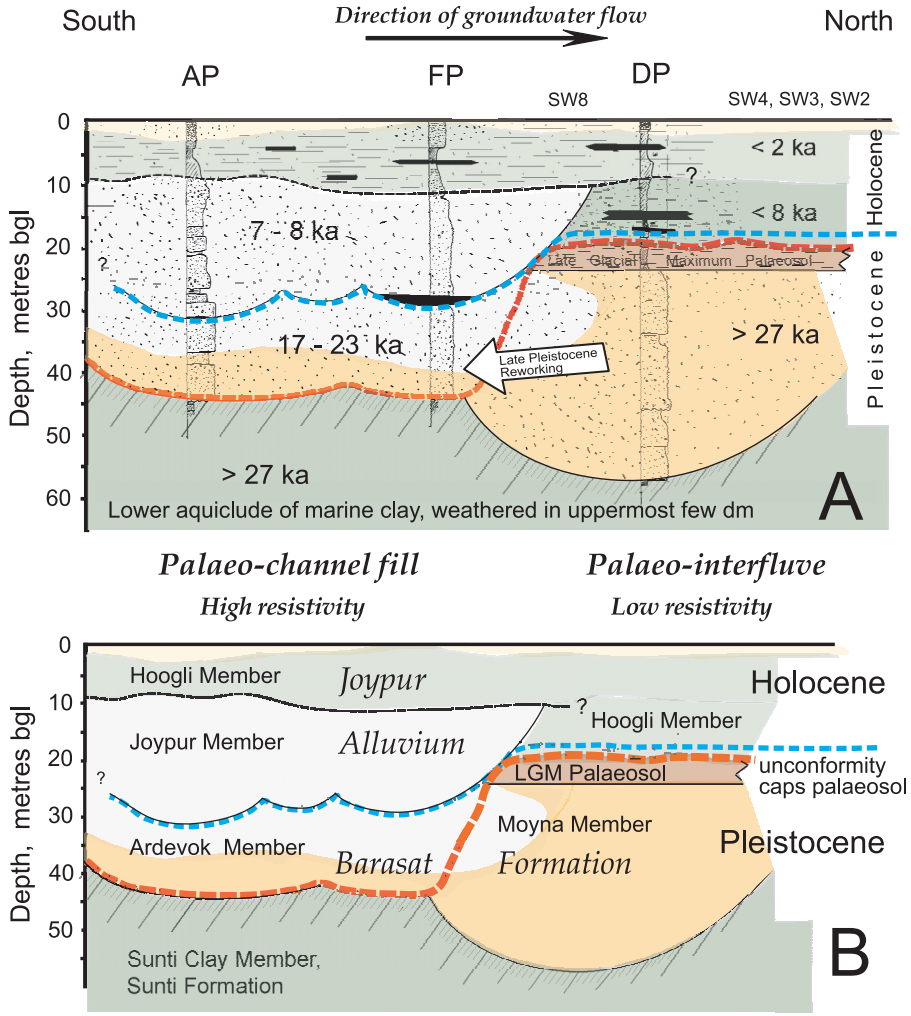

Figure 16. Application in the study area of the regional sedimentological model in Figures 14 and 15, interpreting the lithostratigraphy, sediment dates, and sedimentological units, in terms of paleointerfluve and paleochannel sequences. The dashed red line denotes the level of maximum incision and erosion during the Last Glacial Maximum. The dashed blue line represents the Pleistocene-Holocene transition; its location is above the LGMP but below the deepest sediment dated at DP, which was at 16.8 mbgl. Black stringers are peaty horizons. The pale lobe invading the Moyna Member's southern margin represents an encroaching redox front driven by the northerly flow of groundwater; see Figure 18 and text for a fuller account.

onto unreduced MnO_2 and FeOOH in the brown sands of the Monya Member. Experimental sorption studies, and modeling of the retardation of dissolved arsenic by brown Pleistocene sand from the IDE site on the Jamuna floodplain in Bangladesh, yielded retardation factors for As(V) that were dependent on arsenic concentration, but ranged from about 25, at an arsenic concentration of 900 μg/L, to about 125 at an arsenic concentration of 50 μg/L (recharge rate 1.4 m/a *Stollenwerk et al.* [2007, 6]; porosity 0.33 from K. Stollenwerk (personal communication, 2008). Applied to JAM, these figures would translate into rates of arsenic migration of between 1 and 0.2 m/a. Such migration rates for arsenic might be minimum rates because 95% of the arsenic in the As-polluted parts of the aquifer in JAM is present as As(III) (J. M. McArthur, unpublished data, 2004, 2005). Field experiments by *Höhn et al.* [2006] showed that, under subsurface conditions similar to those found in JAM, As(III) migrates faster than does As(V). Conversely, As(III) migration rates might be slowed by oxidation of As(III) to As(V) by MnO_2 in the aquifer [*Amirbahman et al.*, 2006, and references therein; *Stollenwerk et al.*, 2007], followed by stronger retardation through stronger sorption of the As(V), compared to As(III), to unreduced MnO_2 and FeOOH.

5.4. Numerical Flow Modeling

[59] In order to scope the extent to which the impermeable LGMP protects underlying aquifers from downward flow of groundwater, and so from downward migration of arsenic and organic matter, we have constructed a preliminary model of groundwater flow in our study area. The purpose of the modeling is to underpin our conceptual model of flow, rather than to rigorously quantify flow, as the latter task is beyond the scope of this paper.

[60] We first constructed a single layer horizontal flow model in FLOWPATH® II [*Waterloo Hydrogeologic, Inc.*

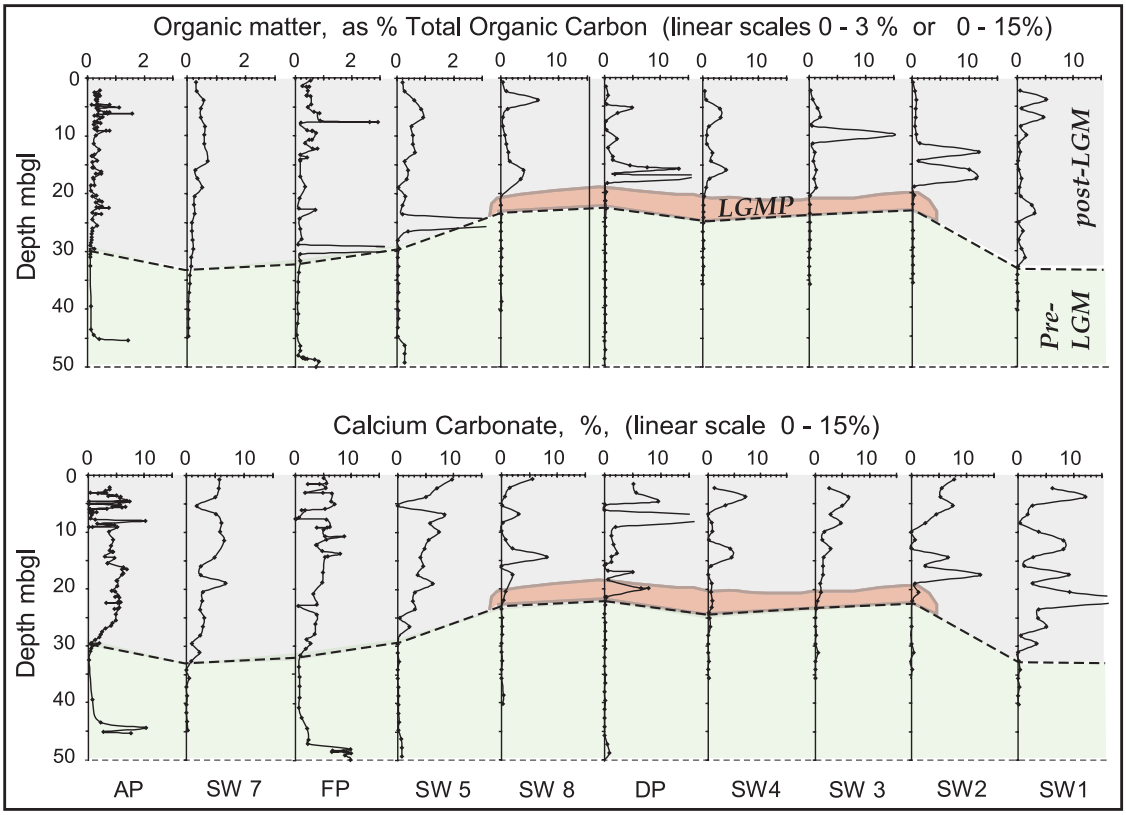

Figure 17. Profiles of TOC and $CaCO_3$ in sediments from JAM. Sites are projected onto a S–N line of traverse that approximates the same line of section as used for Figures 18 and 19. Note that organic-rich sediments are not present at all sites; where present, they appear not to be laterally continuous. An irregular distribution is also seen in $CaCO_3$, enrichments of which may be marking cryptic calcrete horizons.

(*WHI*), 1998] to identify a suitable configuration to use in a multilayer, vertical plane simulation of flow using Visual MODFLOW® 3.0 [*WHI*, 2002]. The FLOWPATH model used measured aquifer permeabilities (30 m/d), and average recharge rates of 100–125 mm/a in order to reproduce the observed piezometry. The MODFLOW model follows the alignment of the NS geological section shown in Figure 3 (essentially along geophysical lines 250E/288E) and extends 1 km south of AP and 1 km north of SW1.

[61] The MODPATH module [*Pollock*, 1994] was used to track the paths of nonreactive particles entering at the water table and on the southern boundary (Figure 19). The model has five layers, and so approximates the sedimentary succession (Figures 2, 3, and 14–17). The top few meters of the upper aquitard were assigned a hydraulic conductivity of 1 m/d to replicate the rapid infiltration observed at DP, and a value of 0.1 m/d, closer to that determined by slug testing, was assigned to the lower part in order to maintain a mound at the water table. The sand of the shallow aquifer was also divided into two layers to allocate abstraction sensibly to depth. The LGMP was assigned a vertical hydraulic conductivity of 10^{-5} m/d. Abstractions from hand-pumped tube wells in the villages were estimated from the number of wells and estimated per capita water consumption. Abstractions from irrigation wells were estimated from irrigation water requirements, as described before. The southern boundary of the model was defined as a General Head boundary that generates a head-dependent lateral flow from the south, capturing the regional flow regime, and with a small downward head difference of 95.7 to 95.4 m above site datum (asd) between the top and bottom layers. The northern boundary was simulated as a fixed head boundary (93 m asd). The northern and southern boundaries were not well constrained by borehole information, but their distances from the investigated area were tested by sensitivity analysis, and judged not to be critical.

[62] The model was run in steady state, with a constant recharge of 100 mm/a that implicitly takes account of the low permeability of the cultivated soil layer and plough pan [*Brammer*, 1996]. Rigorous calibration was made difficult by the limited availability of piezometric data, and the uncertainty surrounding abstraction estimates and the northern boundary condition. Nevertheless, the observed piezometry was effectively simulated using the measured aquifer geometry, and hydraulic properties and recharge rates consistent with regional experience [*Ravenscroft*, 2003, and references therein].

[63] The simulated pattern of flow lines is strongly influenced by the low permeability of the LGMP, and the abstraction by the irrigation wells. Of particular note is the concentration of flow lines at the southern tip of the LGMP, where water recharged over nearly half of the model length

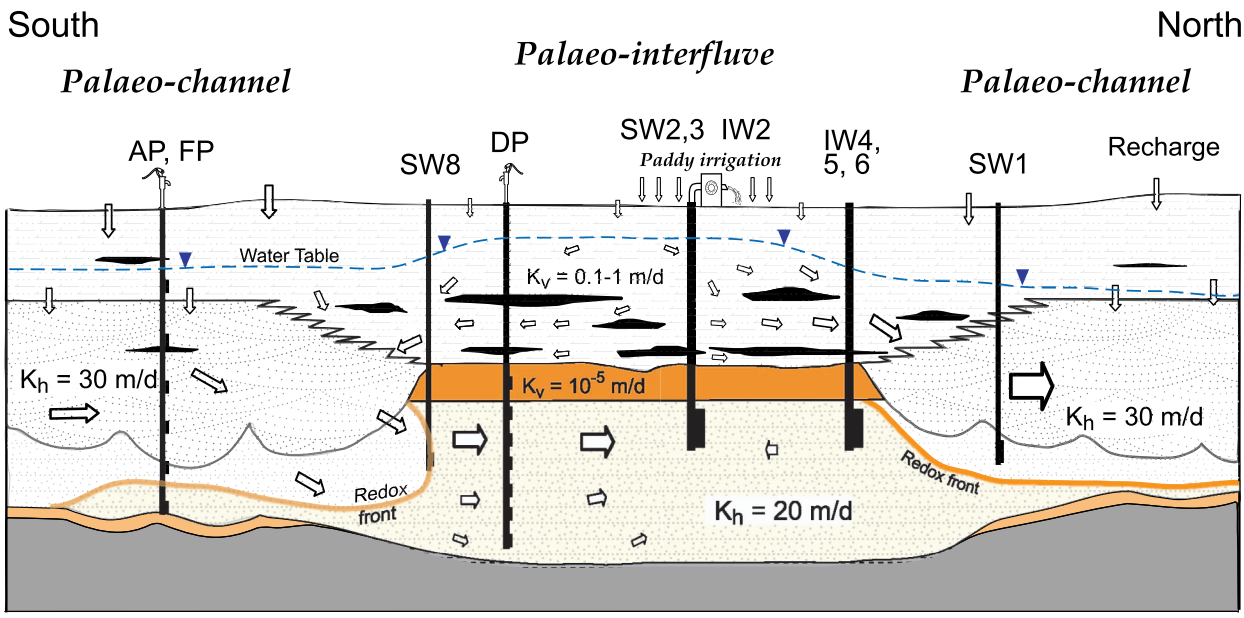

Figure 18. Conceptual model of flow in the shallow aquifer. Rate of groundwater flow is approximated by the size of the open arrows. Groundwater flow in the shallow aquifer is to the north-northeast, from the As-polluted paleochannel regions of southern JAM (zone 3 of Figure 8) northward to the low-As region (zone 1 of Figure 8) beneath the LRZ and LGMP. In this figure, we do not differentiate the Joypur and Ardevok members, as they are hydraulically well connected. The northerly flow of groundwater carries with it As and organic matter to pollute and reduce the aquifer sediments beneath the LRZ. The reduction front represented here is for the total reduction of FeOOH on sediment grains and thus for As release and As pollution. This state is reached at SW8, where the groundwater is rich in Fe and As but is not yet reached at IW4, IW5, and IW6, where FeOOH reduction is occurring, but is incomplete, so the waters are Fe rich but contain only a small amount of As (Table 3). In the center of the LRZ, groundwaters are poised at MnO_2 reduction and contain little As or Fe but much Mn.

converges. At this point, water moving southward along the upper part of the upper aquitard is drawn down below the LGMP and changes direction to flow north. In the Moyna Member, irrigation wells limit the downward movement of groundwater, a prediction consistent with the fact that vertical hydraulic gradients in the lower part of the shallow aquifer are immeasurably small or zero.

[64] About half of the agricultural area in the north of the study region (Figure 1) has been irrigated for upward of 30 years by groundwater from irrigation wells at DIW1 and DIW2 (Figure 1) that tap the deep aquifer at 175 m. In addition, for up to 16 years, shallow irrigation wells tapping the Moyna Member have supplied discrete smallholdings, each comprising a dozen or so fields. This irrigation water must make a significant contribution to recharge in the shallow aquifer. Both the modeling and our conceptual model require recharge, including irrigation returns, to roll over the edge of the LGMP, and be drawn down into the confined aquifer beneath the paleointerfluve. The flow, and the dissolved organic matter that this rollover must carry, has a considerable effect on the brown sands of the Moyna Member, as we show in section 5.5, and the effect is likely to be widespread in the Bengal Basin.

[65] Numerical modeling thus provides verification of the conceptual model described here and demonstrates, among other things, first, the effect of the permeability contrast between the low-permeability Holocene muds and the impermeability of the LGMP; second, the locally focused vertical flows, and rollovers, at the edges of the LGMP; finally, the quantitative importance of horizontal inflow to the confined aquifer underlying the LGMP.

[66] Although beyond the scope of our investigations, we note that the pattern of horizontal and vertical flows around the LGMP is likely to be similarly controlled in the deep aquifer by other paleosols that developed during lowstands of sea level prior to 125 ka. Such multiple paleosols in toto [*Kraus*, 1999, Figures 1 and 5] will have created an anastomosing network of pathways that connect shallow, intermediate and deep aquifers across the Bengal Basin (and in deltas worldwide) and will give the deeper aquifers overall properties that differ from the averaged, continuous layer, properties assumed for use in most groundwater flow models.

5.5. Aquifer Sustainability: The Implications of Abstraction

[67] Where groundwater within the shallow aquifer is tapped from gray sand, the water is rich in arsenic and iron, showing that the aquifer has reached the stage of FeOOH reduction. Where groundwater is tapped from brown sand, it contains little arsenic (mostly <10 μg/L) or iron, and mg/L amounts of manganese, showing that the aquifer is poised at MnO_2 reduction. A continuum of states between these end-members exists, as shown by the lower part of the piezometer profile at AP (Figure 9). The system is dynamic, so the state we see today is but a snapshot of an ever-changing situation. The Ardevok Member was originally brown sand that was reworked from the Moyna Member, so its reduc-

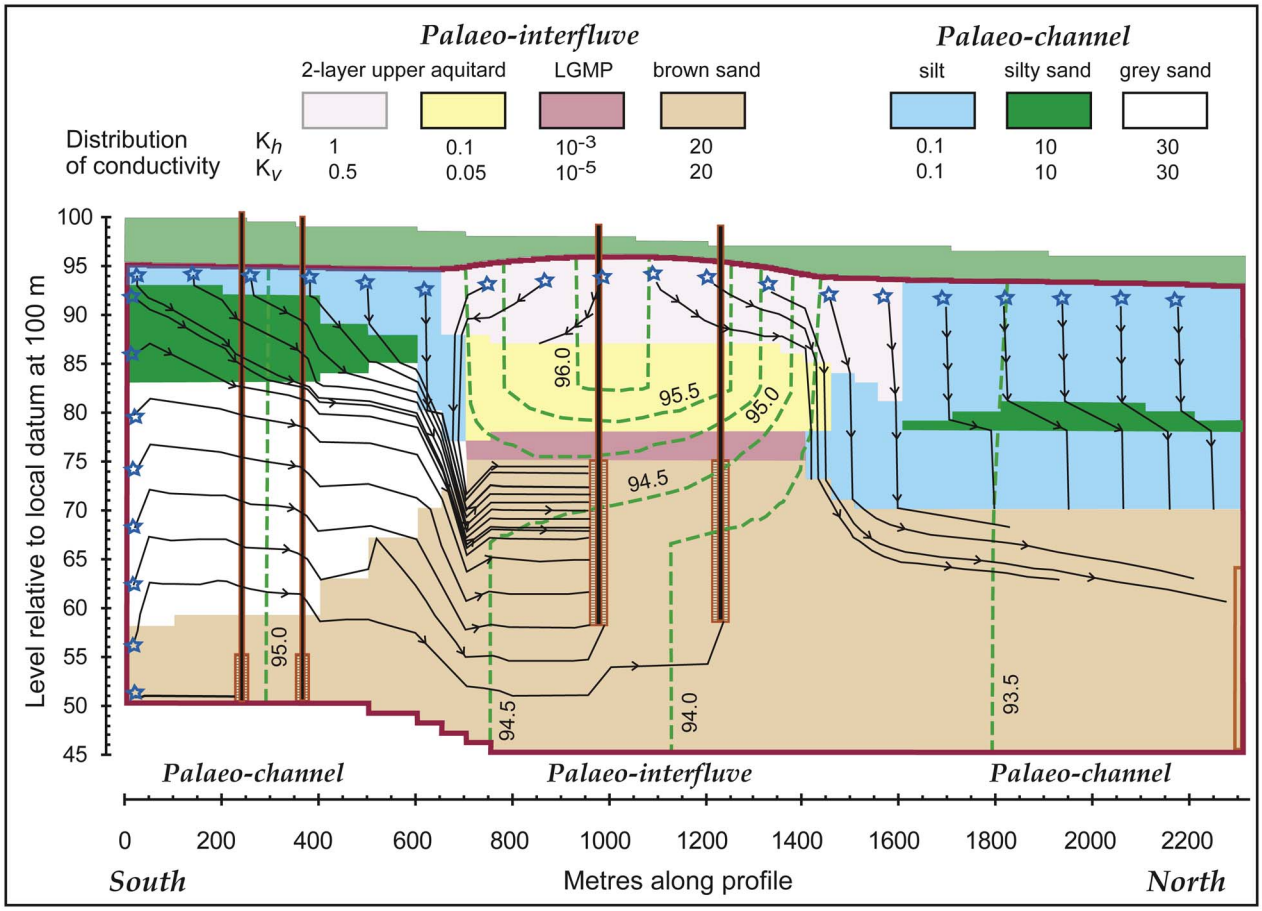

Figure 19. MODFLOW simulation of groundwater flow along a N–S flow path, from 1 km south of AP to 1 km north of SW1 (see Figure 1 for well locations). Profile line approximates the line along AP-SW7-DP-SW3-SW2-SW1 in Figure 1. Black lines are point tracks of particle movement (original position shown by stars); arrows on tracks are at intervals of 10 years. The model was run for 50 years, so some tracks end abruptly. Green dashed lines are contours of hydraulic head, relative to an arbitrary local datum set at 100 m. Colors denote units of differing hydraulic conductivity.

tion has been accomplished by a downward moving reduction front. This front will, given time, reduce the entire sediment column, as has almost happened at FP (Figure 2) where, we speculate, downward moving reduction has been promoted by leakage of labile organic matter from the organic-rich unit at 29.5 m in FP (an example of aquitard diffusion). These examples suggest that wells screened in the lower part of paleochannel aquifers, a strategy adopted by some to avoid pollution from arsenic, are vulnerable to both the drawdown of arsenic from local abstraction and drawdown of dissolved organic carbon that will promote local reduction and aggravate that pollution.

[68] Arsenic pollution will also be spread by horizontal movement of groundwater. Groundwater polluted by arsenic is moving laterally (northward) from polluted aquifers in the south into the unpolluted brown Pleistocene sand of the Moyna Member beneath the LRZ. The water must carry with it dissolved organic matter and must generate a redox front that is also moving northward, thereby generating additional pollution. At least some of this organic matter will be carried by organic-rich water rolling over the edge of the LGMP to recharge the underlying brown sand aquifers.

[69] To illustrate this invasive migration of arsenic, but more centrally this organic matter, into the paleointerfluvial area in JAM, we consider the composition and the redox state of the Moyna Member and its groundwater at four locations. The locations (Figure 8) are (1) in the center of the LRZ (IW2, SW3, SW4); (2) marginal in the LRZ, but still well inside it (DP); (3) close to the northern margin of the LRZ (IW4, IW5, IW6); and (4) on the very edge of the LRZ (SW8). Reduction at these sites has arrived at different stages along the continuum between MnO_2 reduction, FeOOH reduction without As release, and FeOOH reduction with As release, a matter summarized in Figure 20.

[70] 1. In the center of the LRZ at IW2, SW2, SW3, the aquifer sediments are brown over the entire depth drilled (Figures 2 and 18) and groundwaters contain <2 μg/L of arsenic, <0.4 mg/L of iron, and ≥ 2.9 mg/L of manganese. The sediments are poised at MnO_2 reduction. We postulate that this is because sources of organic matter to reduce them are remote; such organic matter cannot penetrate the con-

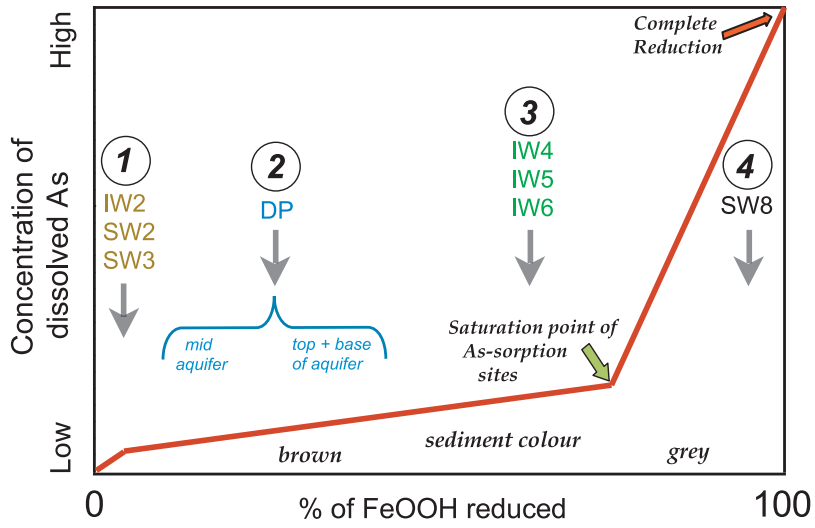

Figure 20. Conceptualization of the redox states seen in JAM at differing locations beneath the LRZ, in terms of the reduction and resorption model of *Welch et al.* [2000] as visualized by *McArthur et al.* [2004]. Sites 1–4 are described in the text and represent redox states from slight reduction of MnO_2 (site 1) to complete reduction of FeOOH (site 4).

fining LGMP, so would need to travel hundreds of meters laterally through brown sand to arrive at the wells, so little has done so.

[71] 2. At DP, nearer to the edge of the LRZ, the aquifer is still oxidized and brown over the entire depth drilled (Figures 2 and 18). In the middle part (most) of the aquifer, redox is poised at MnO_2 reduction and concentrations of arsenic (<2 μg/L), iron (<1 mg/L) and manganese (>2 mg/L) in groundwater reflect that fact (Figure 9). At the top and base of the aquifer, a change toward FeOOH reduction is apparent as manganese concentrations are lower, and iron concentrations higher, than in the aquifer's center; nevertheless, arsenic concentrations remain low ($\leq$5 μg/L) owing to resorption of arsenic, released by minimal FeOOH reduction, to unreduced MnO_2 and/or FeOOH. We conclude that the distal end of the encroaching redox front is beginning to impact the top and base of the aquifer at DP, but its presence is not strong. The proximal edge of the redox front appears to be a few tens of meters to the south of DP, at well Ba 13 (Figure 8), which increased its concentration of arsenic linearly from 32 to 113 μg/L between February 2003 and February 2008.

[72] 3. A more advanced stage of redox development, beyond that seen at the top and base of DP, is apparent at IW4, 5, and 6 (Figure 8). The groundwaters contain 8–11 mg/L of iron (Table 3), 1–2 mg/L of manganese, and significant, but low, amounts of arsenic (28–87 μg/L). These sites are nearer the edge of the LRZ than is DP. Near IW4, 5, and 6, we infer that groundwater, having passed through the organic-rich upper aquitard where it acquired dissolved organic matter, rolls over the edge of the LGMP and enters the brown sands beneath the LGMP in response to abstraction from these wells near the edge of the LRZ. The presence of such high concentrations of iron, and significant amounts of arsenic, shows that a significant proportion of the FeOOH in the aquifer has been reduced. The arsenic represents that released by reduction of FeOOH but present in solution transiently (Figure 20; the kinetic arsenic of *McArthur et al.* [2004]) before resorption to residual FeOOH, as predicted by the dissolution model of *Welch et al.* [2000]. The amount of reduction is beginning to approach that at which residual FeOOH reaches saturation with sorbed arsenic, but reduction is not yet sufficient for arsenic to appear in solution in large amounts

[73] 4. Well SW8, on the edge of the LRZ (Figures 3, 5, 6, and 8), is the most polluted well in JAM; it contains 1410 μg/L of arsenic, 9 mg/L of iron, and 0.1 mg/L of manganese. The lithological profile at SW8 is similar to that at SW2, 3 and 4, in that peat and thick silt overlie the LGMP, but SW8 differs in that only the top 2 m of sand is brown and FeOOH bearing; brown sand passes gradationally into gray sand between 2 and 5 m from the top of the aquifer. This is the only site where brown sand overlies gray sand. At SW8, the extremely high concentrations of arsenic in the groundwater, and a distribution of sediment color (i.e., FeOOH) that is uncharacteristic of its sedimentary succession, show that FeOOH reduction has gone largely to completion. As reduction proceeded, FeOOH would have became loaded to saturation with sorbed (and resorbed) arsenic as predicted by the reduction model of *Welch et al.* [2000] (Figure 20). The continuing reduction of FeOOH beyond that stage is therefore releasing a maximal load of sorbed (and resorbed) arsenic to solution. It is the proximity of SW8 to the edge of the LGMP, and so the proximity to the organic-rich groundwater rolling over the edge of the LGMP, that has permitted this to happen.

[74] In summary, the risk of arsenic pollution is primarily proportional to the distance of the well from the edge of the LGMP. The risk of pollution in the Moyna Member is greatest on the edge of the LRZ, i.e., at the limit of the protecting LGMP, and risk is least centrally within the LRZ. That risk will be modified by vertical and horizontal flows induced by pumping from beneath the LRZ. In the area of JAM upgradient of the pumping well, this local pumping will increase the northerly flow induced by regional abstraction of groundwater; in the region downgradient of the pumping well, the northerly regional flow will be decreased or reversed (Figure 18).

5.6. Color and Age of Sediments

[75] Since the first report that brown Pleistocene sands in Bangladesh are rarely, if ever, polluted by arsenic [*DPHE*, 1999], the association between brown sands and low arsenic concentrations has been widely confirmed [*Pal et al.*, 2002; *van Geen et al.*, 2003; *McArthur et al.*, 2004; *von Brömssen et al.*, 2007]. This has lead to a common perception that, in the Bengal Basin, drilling through the Holocene cover into pre-LGM sands will provide low-arsenic water because the Pleistocene brown, oxidized sands contain iron oxyhydroxide to buffer reduction and retard migration of arsenic. Although that is broadly correct, our investigations show that the situation is more complex. Where the Pleistocene brown sands are not protected from downward movement of water by the LGMP, they are vulnerable to pollution not only by invasion of arsenic-rich water, but also from invasion by organic matter and so reduction of FeOOH which will lead to additional pollution. Where that has happened, the sediments will have been reduced and the gray color will not indicate a Holocene age. At the paleochannel sites (particularly at FP), most or all of the 12–14 m of Pleistocene sand underlying the Holocene sand has now been partially or completely reduced, is gray in color, and is polluted by arsenic: to what extent this is a response to natural flow, or to abstraction of groundwater, we cannot say. We note, however, that ^{14}C dates on sediment obtained from the upper part of the upper aquitard are around 2000 years (Table 1), suggesting that the Holocene sand became isolated from atmospheric oxygen no later than that time. Confinement, and so isolation from the atmosphere, rapidly drives groundwater to the anoxic state, promoting reduction, which would have migrated downward and laterally from the source of organic matter in the upper aquitard. Before confinement, it is likely that groundwater in the sands would have been oxic and arsenic free.

[76] For some years, residents of Ardevok living around piezometer nest AP (zone 3 of Figure 8) have sited wells on the basis of sand color, a strategy noted by *McArthur et al.* [2004]. This principle has been advocated by *von Brömssen et al.* [2007, p. 121] who suggest "that sediment color is a reliable indicator of high- and low-As concentrations and can be used by local drillers to target low-arsenic groundwater." As a guide to short-term performance of new wells, the principle is useful. However, our results suggest that this will be an unreliable guide to long-term performance. Long-term planning should incorporate an understanding of sediment architecture, especially of interfluvial and paleochannel sequences, and recognize that paleointerfluves are discontinuous. For maximum protection, tube wells should be sited well inside the boundaries of regions of paleointerfluvial brown sands, and off center and down gradient of the invasion edge, or at some minimum distance below the gray-brown interface in paleochannel sequences [cf. *Stollenwerk et al.*, 2007].

[77] The size and continuity of interfluvial areas is unknown. They need to be defined through mapping of the distribution of arsenic in groundwater. The task may be aided by shallow-resistivity surveying. By delineating paleointerfluvial areas across the Bengal Basin, and combining their use in irrigation with piped supplies of potable water drawn from deep wells, a substantial mitigation might be achieved of arsenic pollution of both potable water and agricultural soil. Such a solution has the advantage of being community based (localized) rather than being dependent on pipelines to supply water from treated, probably distant, sources. This solution would also avoid the disadvantage that paleointerfluvial areas beneath a LGMP may yield water with high concentrations of manganese; up to 3 mg/L is not uncommon. This is some 7 times the WHO guideline value [*World Health Organization*, 2004] and such concentrations may affect the health of young consumers [*Wasserman et al.*, 2006]. Inversely, the relation of high manganese and interfluvial areas of the Bengal Basin noted here may provide a framework for understanding the extent and severity of manganese contamination of groundwater.

5.7. LGMP Across the Bengal Basin

5.7.1. Point Identification of the LGMP

[78] Outside our study area, Late Pleistocene paleosols have been found at depths of a few tens of meters in many parts of Bangladesh: on the Jamuna Floodplain [*Coleman*, 1969; *Davies*, 1994; *BADC*, 1992]; the Old Brahmaputra Floodplain [*BADC*, 1992; *Zheng et al.*, 2004]; the Meghna Floodplain [*Yount et al.*, 2005]; and at locations across southern Bangladesh by *Goodbred and Kuehl* [2000a]. In the Bengal Basin, this LGMP is therefore apparently widespread, but discontinuous. Additionally, in Matlab, in SE Bangladesh, the LGMP appears to be present over brown sand at a depth of 35–40 mbgl at two sites investigated by *von Brömssen et al.* [2007], but is not clearly present at their third. On the Jamuna floodplain in central Bangladesh, *Stollenwerk et al.* [2007], reported a Holocene paleochannel sequence of gray sand overlying brown Pleistocene sand. The two units may be separated by a clayey sand at the base of the Holocene unit, but their hydraulic relation is not resolved.

5.7.2. Areal Identification of the LGMP

[79] The relations between sedimentology, arsenic distribution, groundwater flow, and the LGMP, are not clear from the studies mentioned in section 5.7.1 because arsenic pollution in groundwater was not mapped in the immediate vicinity of those sites. That was done, however, in West Bengal by *Pal et al.* [2002] at Baruipur, some 60 km south of Kolkata in West Bengal, in 24-Parganas South, an area severely affected by arsenic pollution. These authors found that low-arsenic water underlay areas a few hundred meters in lateral extent in which the sedimentary sequence comprised peaty sediment around 20–25 m in thickness over an aquifer of brown sand. Under surrounding areas lay arsenical water beneath a thinner, peat-free upper aquitard. The far field, not investigated sedimentologically, was also low in arsenic. From the account given by those authors, that region appears to be a close analog of ours, with the low-arsenic areas representing paleointerfluves and the high-arsenic areas representing paleochannels.

5.7.3. Competitors to the LGMP for Controlling Groundwater Flow

[80] In focusing on the LGMP, we do not discount the fact that other impermeable strata are present in the Bengal Basin. Such units are common, e.g., overbank clays and swamp deposits, the latter often organic rich and even peaty. Three differences mark out the LGMP from such strata. The first is that the LGMP caps, i.e., physically sits upon, the brown sands of the paleointerfluves; no sediments intervene between the LGMP and the brown sands to lessen

the protection the LGMP affords. Other low-permeability strata are at lesser depths, are not in direct contact with the underlying paleointerfluvial sands, and so cannot afford the same degree of protection from vertical migration of arsenic and organic matter.

[81] The second difference is that the LGMP, although somewhat time transgressive, formed everywhere by the same process and so should be present basin wide. The LGMP formed everywhere, except in active river channels, because it formed in response to a global driver, the glacioeustatic lowering of sea level between 125 ka and 20 ka. It is the scale and continuity of the LGMP that makes it so important in controlling groundwater flow.

[82] Other low-permeability strata overlying the LGMP would have formed in response to sedimentological processes operating on an aggrading alluvial delta and would necessarily be of more limited lateral extent. Such strata are heterogeneous in age and distribution. While locally impeding flow, they are unlikely to be laterally extensive (certainly not basin wide), and may be disrupted by later, even modern, channel avulsion. In our area, the profiles of TOC and $CaCO_3$ across the study area show the presence of such horizons, especially peats (Figure 17). These profiles emphasize the lateral discontinuity of such units; the levels rich in TOC or $CaCO_3$ are found at differing depths in differing parts of the study area.

[83] Finally, being a paleosol, the LGMP has definite characteristics that should be seen basin wide, not least its red/orange color and its content of carbonized rootlets. These characteristics should make the LGMP identifiable in the field. Once located in a region, its depth will be predictable locally because of the generic nature of the unit, and that predictability will be of value when siting new wells and generally in aquifer exploitation.

5.8. LGMP Worldwide

[84] Between 125 ka and the Last Glacial Maximum around 20 ka, sea level fell by around 120 m [*Lambeck et al.*, 2002]. The falling sea level caused incision of paleochannels and paleosol development (the LGMP) on the interfluves. Glacioeustatic changes in sea level are global, so the LGMP should be found, in a range of preservational states, in many deltas of the world. It seems likely that control of flow by an equivalent of our LGMP will be found in other deltaic aquifers worldwide where hinterland geology has permitted the development in the delta of extensive fluvial sands to act as aquifers. Where those deltaic aquifers are polluted by arsenic, the LGMP will influence the distribution of pollution. As mean annual precipitation is a strong control on the formation of paleosol clays (and so impermeability) the effect of paleosols on groundwater flow will be particularly strong where rainfall is high, such as in tropical regions and monsoonal regions such as Asia.

[85] It is therefore no surprise that the LGMP appears to have equivalents in western India [*Bhandari et al.*, 2005], the Red River (Song Hong) Basin of Vietnam [*Tanabe et al.*, 2003, Figure 2; *Hanebuth et al.*, 2006; *Funabiki et al.*, 2007], and the Po Valley of Italy [*Amorosi et al.*, 2003] where arsenic pollution is extensive [*Giuliano*, 1995; *Agenzia Regionale Prevenzione e Ambiente dell Emilia-Romagna*, 2005]. It is also widespread in settings that are now shallow marine, but which were exposed subaerially during the LGM, such as the floor of the Yellow Sea off western Korea [*Lim et al.*, 2004; *Choi*, 2005], the northern South China Sea [*Yim et al.*, 2004] and the Sunda Shelf [*Hanebuth and Stattegger*, 2004]. The prevalence of paleosols in deltaic settings is clear from the review of paleosol formation by *Kraus* [1999, and references therein].

[86] The LGMP in the Red River (Song Hong) Basin is particularly pertinent. The shallow alluvial aquifers around Hanoi are polluted by arsenic [*Berg et al.*, 2001] and the As-polluted groundwater is similar in composition to As-polluted groundwater in the Bengal Basin [*McArthur et al.*, 2004]. The LGM in the Red River Basin is marked by prominent paleosols recognized in cores [*Hanebuth et al.*, 2006; *Funabiki et al.*, 2007], and the LGM surface appears as a unit on the geological map of the region presented by *Tanabe et al.* [2003], on which it appears to crop out away from the subsidence center of the basin, on peripheral higher ground. On the basis of our model, we predict that the geographical distribution of arsenic pollution in the Red River Basin will be fractal at most scales, as it is in the Bengal Basin. We further predict that it will be controlled by the same paleochannel and paleointerfluve relations as we document in the Bengal Basin. Unpolluted shallow aquifers should exist beneath local and regional equivalents of the LGMP, while polluted aquifers will occupy paleochannels; groundwater flow will be strongly focused and controlled by the LGMP in a manner similar to that shown in our conceptual and numerical models.

6. Conclusions

[87] The aquifer sediments of the study area comprise two sequences that are likely, subject to local modifications introduced by differing climates and hinterland elevations, to characterize deltaic aquifers worldwide: (1) a paleochannel sequence, in which gray Holocene sand directly overlies gray-to-brown Pleistocene sand, the gray sands in both of which contain groundwater that is polluted by arsenic; and (2) a paleointerfluve sequence where peaty, Holocene, silts overlies a Late Pleistocene paleosol, which in turn caps brown Pleistocene sands in which groundwater is not polluted by arsenic. We term the paleosol the Last Glacial Maximum paleosol (LGMP) because it formed by weathering of brown, oxidized, Pleistocene sediments as sea level fell between 125 ka and the lowstand at 20 ka known as the Last Glacial Maximum.

[88] In the paleointerfluves, the LGMP prevents the downward flow of groundwater into underlying brown Pleistocene sands and so protects them from downward moving arsenic, and from downward migrating organic matter which would drive FeOOH reduction and add to As pollution. In the paleochannel sequence, where the LGMP is absent, there is good hydraulic continuity between the Pleistocene sands and overlying Holocene sands. Arsenic, mobilized by the degradation of Holocene organic matter in the upper aquitard and locally within the Holocene sand (e.g., at 29 m in FP), migrates downward to pollute underlying brown Pleistocene sands. It is accompanied by organic matter that promotes FeOOH reduction and so aggravates As pollution.

[89] Groundwater polluted by arsenic is migrating laterally at depth through the paleochannel sands into the paleointerfluvial brown Pleistocene sands. Hydraulic and modeling evidence suggests lateral migration of water of the

order of 30 m/a, with arsenic moving at around 0.2 to 1 m/a owing to sorption to FeOOH. Further monitoring and reactive transport modeling are required to quantify this migration rate better, and so provide an accurate prognosis of the likely period over which the unpolluted paleointerfluvial aquifers will deliver low-As groundwater.

[90] In our area, electrical resistivity surveys provide guidance on where in the subsurface low-arsenic water is likely to be found at shallow depth because low apparent resistivity corresponds to the paleointerfluve (low-arsenic) sequence, and higher resistivities correspond to the paleochannel (As-polluted) sequence. Further testing of this association should be undertaken elsewhere in the Bengal Basin to establish the wider potential of shallow resistivity surveys in this regard.

[91] Our general concept is of paleochannel sequences dissecting a buried, paleosol-capped, Pleistocene landscape, all covered by a rapidly deposited and laterally extensive Holocene interfluvial sequence that may be muddy (as at our site) or sandy. This conceptual model should be widely applicable in the Bengal Basin, and probably elsewhere. The sedimentological aspect of the model is neither original nor surprising; see, for example, the documentation of paleochannels and paleointerfluves in the Yangtze Delta by *Li et al.* [2000]. Despite this familiarity, a paleosol model (one that invokes control of flow from a single, generic, unit that is basin wide) has not been applied to hydrogeological thinking in relation either to the Bengal Basin or more widely, or to the distribution of arsenic pollution anywhere. The model requires a change in the conceptualization of pollutant migration away from the idea of diffuse, laterally extensive, downward leakage extrapolated from measurements at single profiles, toward the idea that vertical flow is concentrated in high-permeability zones that are separated by extensive areas where horizontal flow dominates. The zones of vertical flow may be difficult to locate. Application of this conceptual model may explain the difficulty of apparently calibrated hydraulic models to correctly predict the migration of arsenic, salinity, and other pollutants.

[92] **Acknowledgments.** Arsenic analysis was done courtesy of NERC Central Services; we thank Benoit Disch for assistance with the work. We thank the inhabitants of Joypur, Ardevok, and Moyna for access to their wells, Azizul Fakir for assistance with logistics, and Ali Ahmed Fakir, D. Chandra Ghatak, and Dual C. Shee for permission to install piezometers on their land. Funding for this work was provided by NERC (grant GR8/04292 to K.A.H.-E.), the Birkbeck Faculty of Science (K.A.H.-E.), the Royal Society (J.M.M.), the British Council-UGC (New Delhi) via a Higher Education LINK Scheme grant to Delhi University and UCL, and Research Studentships to S. Sengupta and R. Purohit. The authors thank Ondra Sracek, Douglas Kent, Tom Torgersen, and one anonymous reviewer for comments that substantially improved the script.

References

Agenzia Regionale Prevenzione e Ambiente dell Emilia-Romagna (2005), Presenza e diffusione dell'arsenico nel sottouolo e nelle risorse idriche Italiane: Nuovi strumenti di valutazione dinamiche di mobilizzazione. I quaderni di Arpa, 213 pp., Bologna, Italy.

Ali, M. (2003), Review of drilling and tube well technology for groundwater irrigation, in *Groundwater Resources and Development in Bangladesh—Background to the Arsenic Crisis, Agricultural Potential and the Environment*, edited by A. A. Rahman and P. Ravenscroft, pp. 197–233, Univ. Press, Dhaka.

Allison, M. A., S. R. Khan, S. L. Goodbred Jr., and S. A. Kuehl (2003), Stratigraphic evolution of the late Holocene Ganges-Brahmaputra lower delta plain, *Sediment. Geol.*, *155*, 317–342, doi:10.1016/S0037-0738(02)00185-9.

Amirbahman, A., D. B. Kent, G. P. Curtis, and J. A. Davis (2006), Kinetics of sorption and abiotic oxidation of arsenic(III) by aquifer materials, *Geochim. Cosmochim. Acta*, *70*, 533–547, doi:10.1016/j.gca.2005.10.036.

Amorosi, A., M. C. Centineo, M. L. Colalongo, G. Pasini, G. Sarti, and S. C. Vaiani (2003), Facies architecture and latest Pleistocene-Holocene depositional history of the Po Delta (Comacchio area), Italy, *J. Geol.*, *111*, 39–56, doi:10.1086/344577.

Bailey, R. M., S. Stokes, and H. E. Bray (2003), Inductively coupled plasma mass spectrometry ICP-MS for dose rate determination: Some guidelines for sample preparation and analysis, *Ancient TL*, *21*, 11–15.

Banerjee, M., and P. K. Sen (1987), Palaeobiology in understanding the change of sea level and coastline in Bengal basin during Holocene period, *Indian J. Earth Sci.*, *14*, 307–320.

Bangladesh Agricultural Development Corporation and Overseas Development Administration (BADC) (1992), Final report of the Deep Tubewell II Project, vol. 2.1, Natural resources, Dhaka.

Berg, M., H. C. Tran, T. C. Nguyen, H. V. Pham, R. Schertenleib, and W. Giger (2001), Arsenic contamination of ground and drinking water in Vietnam: A human health threat, *Environ. Sci. Technol.*, *35*, 2621–2626, doi:10.1021/es010027y.

Berner, R. A., and R. Raiswell (1984), C/S method for distinguishing freshwater from marine sedimentary rocks, *Geology*, *12*, 365–368, doi:10.1130/0091-7613(1984)12<365:CMFDFF>2.0.CO;2.

Bhandari, S., D. M. Maurya, and L. S. Chamyal (2005), Late Pleistocene alluvial plain sedimentation in Lower Narmada Valley, western India: Palaeoenvironmental implications, *J. Asian Earth Sci.*, *24*, 433–444, doi:10.1016/j.jseaes.2003.12.011.

Blum, M. D., and T. E. Törnqvist (2000), Fluvial responses to climate and sea-level change: A review and look forward, *Sedimentology*, *47*, 2–48, doi:10.1046/j.1365-3091.2000.00008.x.

Bouwer, H., and R. C. Rice (1976), A slug test for determining the hydraulic conductivity of unconfined aquifers with completely or partially penetrating wells, *Water Resour. Res.*, *12*, 423–428, doi:10.1029/WR012i003p00423.

Brammer, H. (1996), *The Geography of the Soils of Bangladesh*, Univ. Press, Dhaka.

Bray, H. E., and S. Stokes (2003), Chronologies for Late Quaternary barchan dune reactivation in the southeastern Arabian Peninsula, *Quat. Sci. Rev.*, *22*, 1027–1033, doi:10.1016/S0277-3791(03)00014-3.

Bray, H. E., and S. Stokes (2004), Temporal patterns of arid-humid transitions in the south-eastern Arabian Peninsula based on optical dating, *Geomorphology*, *59*, 271–280, doi:10.1016/j.geomorph.2003.07.022.

Bray, H. E., R. M. Bailey, and S. Stokes (2002), Quantification of cross-irradiation and cross-illumination using a Risø TL/OSL DA-15 reader, *Radiat. Meas.*, *35*, 275–280.

British Standards Institution (1975), Site investigation for engineering purposes, *BS 1377*, London.

Chakraborti, D., M. K. Sengupta, M. M. Rahman, U. K. Chowdhury, D. Lodh, C. R. Chanda, G. K. Basu, S. C. Mukherjee, and K. C. Saha (2003), Groundwater arsenic exposure in India, in *Arsenic Exposure and Health Effects*, edited by W. R. Chappell et al., pp. 3–24, Elsevier, Amsterdam.

Choi, K. (2005), Pedogenesis of late Quaternary deposits, northern Kyonggi Bay, Korea: Implications for relative sea-level change and regional stratigraphic correlation, *Palaeogeogr. Palaeoclimatol. Palaeoecol.*, *220*, 387–404, doi:10.1016/j.palaeo.2005.02.006.

Coleman, J. M. (1969), Brahmaputra river: Channel processes and sedimentation, *Sediment. Geol.*, *3*, 129–239, doi:10.1016/0037-0738(69)90010-4.

Das, D., A. Chatterjee, G. Samanta, B. K. Mandal, T. R. Chowdhury, C. R. Chanda, P. P. Chowdhury, G. K. Basu, and D. Chakraborti (1996), Arsenic in groundwater in six districts of West Bengal, India, *Environ. Geochem. Health*, *18*, 5–15, doi:10.1007/BF01757214.

Davies, J. (1994), The hydrogeochemistry of alluvial aquifers in central Bangladesh, in *Groundwater Quality*, edited by H. Nash and G. J. H. McCall, pp. 9–18, Chapman and Hall, London.

Dhar, R. K., et al. (1997), Groundwater arsenic calamity in Bangladesh, *Curr. Sci.*, *73*, 48–59.

Department of Public Health Engineering (DPHE) (1999), Groundwater studies for arsenic contamination in Bangladesh. Rapid investigation phase, final report, Dhaka.

Department of Public Health Engineering (DPHE) (2001), Arsenic contamination of groundwater in Bangladesh, *BGS Tech. Rep. WC/00/19*, Dhaka.

Funabiki, A., S. Haruyama, N. V. Quy, P. V. Hai, and D. H. Thai (2007), Holocene delta plain development in the Song Hong (Red River) delta, Vietnam, *J. Asian Earth Sci.*, *30*, 518–529, doi:10.1016/j.jseaes.2006.11.013.

Giuliano, G. (1995), Ground water in the Po basin: Some problems relating to its use and protection, *Sci. Total Environ.*, *171*(1–3), 17–27.

Goodbred, S. L., Jr., and S. A. Kuehl (1999), Holocene and modern sediment budgets for the Ganges-Brahmaputra river system: Evidence for highstand dispersal to floodplain, shelf and deep-sea epicentres, *Geology*, *27*(6), 559–562, doi:10.1130/0091-7613(1999)027<0559:HAMSBF>2.3.CO;2.

Goodbred, S. L., Jr., and S. A. Kuehl (2000a), The significance of large sediment supply, active tectonism, and eustasy on margin sequence development: Late Quaternary stratigraphy and evolution of the Ganges-Brahmaputra delta, *Sediment. Geol.*, *133*, 227–248, doi:10.1016/S0037-0738(00)00041-5.

Goodbred, S. L., Jr., and S. A. Kuehl (2000b), Enormous Ganges-Brahmaputra sediment supply, active tectonism, and eustasy on margin sequence development: Late Quaternary stratigraphy and evolution of the Ganges-Brahmaputra delta, *Geology*, *28*, 1083–1086, doi:10.1130/0091-7613(2000)28<1083:EGSDDS>2.0.CO;2.

Goodbred, S. L., Jr., S. A. Kuehl, M. S. Steckler, and M. H. Sarkar (2003), Controls on facies distribution and stratigraphic preservation in the Ganges-Brahmaputra delta sequence, *Sediment. Geol.*, *155*, 301–316, doi:10.1016/S0037-0738(02)00184-7.

Halford, K. J., and E. L. Kuniansky (2002), Documentation of spreadsheets for the analysis aquifer-test and slug-test data, *U.S. Geol. Surv. Open File Rep.*, *02-197*.

Hanebuth, T. J. J., and K. Stattegger (2004), Depositional sequences on a late Pleistocene-Holocene tropical siliciclastic shelf (Sunda Shelf, southeast Asia), *J. Asian Earth Sci.*, *23*, 113–126, doi:10.1016/S1367-9120(03)00100-7.

Hanebuth, T. J. J., Y. Saito, S. Tanabe, Q. L. Vu, and Q. T. Ngo (2006), Sea levels during late marine isotope stage 3 (or older?) reported from the Red River delta (northern Vietnam) and adjacent regions, *Quat. Int.*, *145–146*, 119–134, doi:10.1016/j.quaint.2005.07.008.

Harbaugh, A. W., E. R. Banta, M. C. Hill, and M. G. McDonald (2000), MODFLOW-2000, the U.S. Geological Survey modular ground-water model—User guide to modularization concepts and the ground-water flow process, *U.S. Geol. Surv. Open File Rep.*, *00-92*, 121 pp.

Harvey, C. F., et al. (2006), Groundwater dynamics and arsenic contamination in Bangladesh, *Chem. Geol.*, *228*, 112–136.

Hill, I. G., R. H. Worden, and I. G. Meighan (2000), Geochemical evolution of a palaeolaterite: The Interbasaltic Formation, Northern Ireland, *Chem. Geol.*, *166*, 65–84, doi:10.1016/S0009-2541(99)00179-5.

Höhn, R., M. Isenbeck-Schröter, D. B. Kent, J. A. Davis, R. Jakobsen, S. Jann, V. Niedan, C. Scholz, S. Stadler, and A. Tretner (2006), Tracer test with As (V) under variable redox conditions controlling arsenic transport in the presence of elevated ferrous iron concentrations, *J. Contam. Hydrol.*, *88*, 36–54.

HydroSOLVE (1999), *AQTESOLV for Windows v2.5*, Reston, Va.

Islam, M. S., and M. J. Tooley (1999), Coastal and sea level changes during the Holocene in Bangladesh, *Quat. Int.*, *55*, 61–75, doi:10.1016/S1040-6182(98)00025-1.

Islam, S. M. (2001), *Sea-Level Changes in Bangladesh: The Last Ten Thousand Years*, Asiatic Soc. of Bangladesh, Dhaka.

Kahmann, J. A., J. Seaman, and S. G. Driese (2008), Evaluating trace elements as paleoclimate indicators: Multivariate statistical analysis of Late Mississippian Pennington Formation paleosols, Kentucky, U. S. A., *J. Geol.*, *116*, 254–268, doi:10.1086/587883.

Kraus, M. J. (1999), Paleosols in clastic sedimentary rocks: Their geologic applications, *Earth Sci. Rev.*, *47*, 41–70, doi:10.1016/S0012-8252(99)00026-4.

Kruseman, G. P., and N. A. de Ridder (1992), *Analysis and Evaluation of Pumping Test Data*, 2nd ed., Int. Inst. for Land Reclam. and Impr., Wageningen, Netherlands.

Kudrass, H. R., V. Spiess, M. Michels, B. Kottke, and S. R. Khan (1999), Transport processes, accumulation rates and a sediment budget for the submarine delta of the Ganges-Brahmaputra and the swatch of no ground, Bangladesh, paper presented at Quaternary Development and Coastal Hydrodynamics of the Ganges Delta in Bangladesh, Geol. Surv. of Bangladesh, Dhaka, 20–21 Sept.

Lambeck, K., T. M. Esat, and E.-K. Potter (2002), Links between climate and sea levels for the past three million years, *Nature*, *419*, 199–206, doi:10.1038/nature01089.

Li, C., Q. Chen, J. Zhang, S. Yang, and D. Fan (2000), Stratigraphy and paleoenvironmental changes in the Yangtze Delta during the Late Quaternary, *J. Asian Earth Sci.*, *18*, 453–469, doi:10.1016/S1367-9120(99)00078-4.

Lim, D. I., H. S. Jung, B. O. Kim, J. Y. Choi, and H. M. Kim (2004), A buried palaeosol and late Pleistocene unconformity in coastal deposits of the eastern Yellow Sea, east Asia, *Quat. Int.*, *121*, 109–118, doi:10.1016/j.quaint.2004.01.027.

McArthur, J. M., et al. (2004), Natural organic matter in sedimentary basins and its relation to arsenic in anoxic groundwater: The example of West Bengal and its worldwide implications, *Appl. Geochem.*, *19*, 1255–1293, doi:10.1016/j.apgeochem.2004.02.001.

Murray, A. S., and A. G. Wintle (2000), Luminescence dating of quartz using an improved single-aliquot regenerative-dose protocol, *Radiat. Meas.*, *32*, 57–73, doi:10.1016/S1350-4487(99)00253-X.

Pal, T., P. K. Mukherjee, and S. Sengupta (2002), Nature of arsenic pollutants in groundwater of Bengal basin—A case study from Baruipur area, West Bengal, India, *Curr. Sci.*, *82*, 554–561.

Pollock, D. W. (1994), User's guide for MODPATH/MODPATH-PLOT, version 3: A particle tracking post-processing package for MODFLOW, the U.S. Geological Survey finite-difference ground-water flow model, *U.S. Geol. Surv. Open File Rep.*, *94-464*.

Public Health Engineering Department (1991), Final report, steering committee, Arsenic Investigation Project, 57 pp., Kolkata, India.

Ravenscroft, P. (2003), Overview of the hydrogeology of Bangladesh, in *Groundwater Resources and Development in Bangladesh—Background to the Arsenic Crisis, Agricultural Potential and the Environment*, edited by A. A. Rahman and P. Ravenscroft, pp. 43–86, Univ. Press, Dhaka.

Ravenscroft, P., J. M. McArthur, and B. A. Hoque (2001), Geochemical and palaeohydrological controls on pollution of groundwater by arsenic, in *Arsenic Exposure and Health Effects*, edited by W. R. Chappell, C. O. Abernathy, and R. L. Calderon, pp. 53–77, Elsevier Sci., Oxford, U. K.

Ravenscroft, P., H. Brammer, and K. S. Richards (2009), *Arsenic Pollution: A Global Synthesis*, Blackwell, Malden, Mass.

Saha, K. C., and D. Chakraborti (2001), Seventeen years experience of arsenicosis in West Bengal, India, in *Arsenic Exposure and Health Effects IV*, edited by W. R. Chappell, C. O. Abernathy, and R. L. Calderon, pp. 387–395, Elsevier, Oxford, U. K.

Schumm, S. A. (1993), River response to base level change: Implications for sequence stratigraphy, *J. Geol.*, *101*, 279–294.

Sengupta, S., and A. Sarkar (2006), Stable isotope evidence of dual (Arabian Sea and Bay of Bengal) vapour sources in monsoonal precipitation over north India, *Earth Planet. Sci. Lett.*, *250*, 511–521, doi:10.1016/j.epsl.2006.08.011.

Sengupta, S., J. M. McArthur, A. Sarkar, M. J. Leng, P. Ravenscroft, and D. M. Bannerjee (2008), Do ponds cause arsenic-pollution of groundwater in the Bengal Basin? An answer from West Bengal, *Environ. Sci. Technol.*, *42*, 5156–5164, doi:10.1021/es702988m.

Sharma, S., M. Joachimski, M. Sharma, H. J. Tobschall, I. B. Singh, C. Sharma, M. S. Chauhan, and G. Morgenroth (2004), Holocene paleoclimate reconstruction using multiproxy data from Sanai Lake, central Ganga plain, India, *Quat. Sci. Rev.*, *23*, 145–159, doi:10.1016/j.quascirev.2003.10.005.

Smith, A. H., E. O. Lingas, and M. Rahman (2000), Contamination of drinking-water by arsenic in Bangladesh: A public health emergency, *Bull. World Health Organ.*, *78*, 1093–1103.

Stollenwerk, K. G., G. N. Breit, A. H. Welch, J. C. Yount, J. W. Whitney, A. L. Foster, M. N. Uddin, R. K. Majumder, and N. Ahmed (2007), Arsenic attenuation by oxidized aquifer sediments in Bangladesh, *Sci. Total Environ.*, *379*, 133–150, doi:10.1016/j.scitotenv.2006.11.029.

Stüben, D., Z. Berner, D. Chandrasekharam, and J. Karmakar (2003), Arsenic enrichment in groundwater of West Bengal, India: Geochemical evidence for mobilization of As under reducing conditions, *Appl. Geochem.*, *18*, 1417–1434, doi:10.1016/S0883-2927(03)00060-X.

Stuiver, M., and H. van der Plicht (1998), Editorial comment, *Radiocarbon*, *40*, 12–14.

Stuiver, M., P. J. Reimer, E. Bard, J. W. Beck, G. S. Burr, K. A. Hughen, B. Kromer, G. McCormac, H. van der Plicht, and M. Spurk (1998), INTCAL98 radiocarbon age calibration, 24000–0 cal BP, *Radiocarbon*, *40*, 1041–1083.

Talma, A. S., and J. C. Vogel (1993), A simplified approach to calibrating C-14 dates, *Radiocarbon*, *35*, 317–322.

Tanabe, S., K. Hori, Y. Saito, S. Haruyama, V. P. Vu, and A. Kitamura (2003), Song Hong (Red River) delta evolution related to millennium-scale Holocene sea-level changes, *Quat. Sci. Rev.*, *22*, 2345–2361, doi:10.1016/S0277-3791(03)00138-0.

Umitsu, M. (1993), Late Quaternary sedimentary environments and landforms in the Ganges Delta, *Sediment. Geol.*, *83*, 177–186, doi:10.1016/0037-0738(93)90011-S.

van der Kamp, G. (1976), Determining aquifer transmissivity by means of well response tests: The underdamped case, *Water Resour. Res.*, *12*, 71–77, doi:10.1029/WR012i001p00071.

van Geen, A., et al. (2003), Spatial variability of arsenic in 6000 tube wells in a 25 km^2 area of Bangladesh, *Water Resour. Res.*, *39*(5), 1140, doi:10.1029/2002WR001617.

von Brömssen, M., M. Jakariya, P. Bhattacharya, K. M. Ahmed, M. Z. Hasan, O. Sracek, L. Jonsson, and G. Jacks (2007), Targeting low-arsenic aquifers in Matlab Upazila, southeastern Bangladesh, *Sci. Total Environ.*, *379*, 121–132, doi:10.1016/j.scitotenv.2006.06.028.

Wasserman, G. A., et al. (2006), Water manganese exposure and children's intellectual function in Araihazar, Bangladesh, *Environ. Health Perspect.*, *114*, 124–129.

Waterloo Hydrogeologic, Inc. (WHI) (1998), *FlowPath II for Windows v1.3.2*, Waterloo, Ont., Canada.

Waterloo Hydrogeologic, Inc. (WHI) (2002), *Visual MODFLOW 3.0*, Waterloo, Ont., Canada.

Welch, A. H., D. B. Westjohn, D. R. Helsel, and R. B. Wanty (2000), Arsenic in groundwater of the United States: Occurrence and geochemistry, *Ground Water*, *38*, 589–604, doi:10.1111/j.1745-6584.2000.tb00251.x.

Woolfe, K. J., P. J. Dale, and G. J. Brunskill (1995), Sedimentary C/S relationships in a large tropical estuary: Evidence for refactory carbon inputs from mangroves, *Geo Mar. Lett.*, *15*, 140–144, doi:10.1007/BF01204455.

World Health Organization (2004) Chemical fact sheets: Manganese, in *Guidelines for Drinking-Water Quality: Incorporating First Addendum*, vol. 1, *Recommendations*, 3rd ed., chap. 12, pp. 397–398, Geneva, Switzerland.

Yim, W. W.-S., G. Huang, and L. S. Chan (2004), Magnetic susceptibility study of late Quaternary inner continental shelf sediments in the Hong Kong SAR, China, *Quat. Int.*, *117*, 41–54, doi:10.1016/S1040-6182(03)00115-0.

Yount, J. C., M. Nehal Uddin, S. L. Forman, and J. W. Whitney (2005), Subsurface geology and geochronology studies of deeper aquifers in the Bengal Delta, paper presented at Symposium on the Behaviour of Arsenic in Aquifers, Soils and Plants: Implications for Management, Int. Maize and Wheat Impr. Cent., Dhaka, 16–18 Jan.

Zheng, Y., M. Stute, A. van Geen, I. Gavrieli, R. Dhar, H. J. Simpson, P. Schlosser, and K. M. Ahmed (2004), Redox control of arsenic mobilization in Bangladesh groundwater, *Appl. Geochem.*, *19*, 201–214, doi:10.1016/j.apgeochem.2003.09.007.

D. M. Banerjee and R. Purohit, Department of Geology, University of Delhi, Delhi 110 007, India.

C. Bristow and K. A. Hudson-Edwards, School of Earth Science, Birkbeck University of London, Malet Street, London WC1E 7HX, UK.

J. M. McArthur, J. Milsom, and S. Tonkin, Department of Earth Sciences, University College London, Gower Street, London WC1E 6BT, UK. (j.mcarthur@ucl.ac.uk)

P. Ravenscroft, Department of Geography, University of Cambridge, Downing Place, Cambridge CB2 3EN, UK.

A. Sarkar and S. Sengupta, Department of Geology and Geophysics, Indian Institute of Technology, Kharagpur, West Bengal 721 302, India.